PERGAMON

Chemical Engineering Science 56 (2001) 4517–4535

Chemical Engineering Science

www.elsevier.com/locate/ces

Integrating nonlinear output feedback control and optimal actuator/sensor placement for transport-reaction processes

Charalambos Antoniades, Panagiotis D. Christofides *

Department of Chemical Engineering, University of California, 405 Hilgard Avenue, Box 951592, Los Angeles, CA 90095-1592, USA

Received 28 March 2000; accepted 20 February 2001

Abstract

This paper proposes a general and practical methodology for the integration of nonlinear output feedback control with optimal placement of control actuators and measurement sensors for transport-reaction processes described by a broad class of quasi-linear parabolic partial differential equations (PDEs) for which the eigenspectrum of the spatial differential operator can be partitioned into a finite-dimensional slow one and an infinite-dimensional stable fast complement. Initially, Galerkin's method is employed to derive finite-dimensional approximations of the PDE system which are used for the synthesis of stabilizing nonlinear state feedback controllers via geometric techniques. The optimal actuator location problem is subsequently formulated as the one of minimizing a meaningful cost functional that includes penalty on the response of the closed-loop system and the control action and is solved by using standard unconstrained optimization techniques. Then, under the assumption that the number of measurement sensors is equal to the number of slow modes, we employ a procedure proposed in Christofides and Baker (1999) for obtaining estimates for the states of the approximate finite-dimensional model from the measurements. The estimates are combined with the state feedback controllers to derive output feedback controllers. The optimal location of the measurement sensors is computed by minimizing a cost function of the estimation error in the closed-loop infinite-dimensional system. It is rigorously established that the proposed output feedback controllers enforce stability in the closed-loop infinite-dimensional system and that the solution to the optimal actuator/sensor problem, which is obtained on the basis of the closed-loop finite-dimensional system, is near-optimal in the sense that it approaches the optimal solution for the infinite-dimensional system as the separation of the slow and fast eigenmodes increases. The proposed methodology is successfully applied to a representative diffusion–reaction process and a nonisothermal tubular reactor with recycle to derive nonlinear output feedback controllers and compute optimal actuator/sensor locations for stabilization of unstable steady states.

Keywords: Nonlinear control; Static output feedback control; Optimal actuator/sensor placement; Diffusion–convection–reaction processes

1. Introduction

Transport-reaction processes with significant diffusive and dispersive mechanism are typically characterized by severe nonlinearities and spatial variations, and are naturally described by quasi-linear parabolic partial differential equations (PDEs). Nonlinearities usually arise from complex reaction mechanisms and Arrhenius dependence of the reaction rates on temperature, and spatial variations occur due to the presence of significant diffusion and convection phenomena. Typical examples of transport-reaction processes are tubular reactors, packed-bed reactors, and chemical vapor deposition reactors.

Parabolic PDE systems typically involve spatial differential operators whose eigenspectrum can be partitioned into a finite-dimensional slow one and an infinite-dimensional stable fast complement (Friedman, 1976; Balas, 1979). This implies that the dynamic behavior of such systems can be approximately described by finite-dimensional systems. Therefore, the standard approach to the control of parabolic PDEs involves the application of Galerkin's method to the PDE system to derive ODE systems that describe the dynamics of the dominant (slow) modes of the PDE system, which

* Corresponding author. Tel.: +1-310-794-1015; fax: +1-310-206-4107.

E-mail address: pdc@seas.ucla.edu (P. D. Christofides).

0009-2509/01/$ - see front matter
PII: S0009-2509(01)00123-3

are subsequently used as the basis for the synthesis of finite-dimensional controllers (e.g., Balas, 1979; Ray, 1981). A potential drawback of this approach is that the number of modes that should be retained to derive an ODE system that yields the desired degree of approximation may be very large, leading to complex controller design and high dimensionality of the resulting controllers. Motivated by this, recent efforts on control of parabolic PDE systems have focused on the problem of synthesizing low-order controllers on the basis of ODE models obtained through combination of Galerkin's method with approximate inertial manifolds (see the recent book Christofides, 2001 for details and references).

Even though the developed methods allow to systematically design nonlinear controllers for transport-reaction processes, there is no work on the integration of nonlinear controllers with optimal placement of control actuators and measurement sensors for transport-reaction processes so that the desired control objectives are achieved with minimal energy use. Regarding the problem of optimal placement of control actuators, the conventional approach is to select the actuator locations based on open-loop considerations to ensure that the necessary controllability requirements are satisfied. More recently, efforts have been made on the problem of integrating feedback control and optimal actuator placement for certain classes of linear distributed parameter systems including investigation of controllability measures and actuator placement in oscillatory systems (Arbel, 1981), optimal placement of actuators for linear feedback control in parabolic PDEs (Xu, Warnitchai, & Igusa, 1994; Demetriou, 1999) and in actively controlled structures (Rao, Pan & Venkayya, 1991; Choe & Baruh, 1992).

On the other hand, the problem of selecting optimal locations for measurement sensors in distributed parameter systems has received very significant attention over the last 20 years. The essence of this problem is to use a finite number of measurements to compute the best estimate of the entire distributed state for all positions and times employing a state observer in the presence of measurement noise. Efforts for the solution of this problem have focused on linear systems (Yu & Seinfeld, 1973; Chen & Seinfeld, 1975; Kumar & Seinfeld, 1978a; Omatu, Koide, & Soeda, 1978; Morari & O'Dowd, 1980) and the application of the results to optimal state estimation in tubular reactors (Colantuoni & Padmanabhan, 1977; Kumar & Seinfeld, 1978b; Harris, MacGregor, & Wright, 1980; Alvarez, Romagnoli, & Stephanopoulos, 1981; Waldraff, Dochain, Bourrel, & Magnus, 1998). The central idea to the solution involves the use of a spatial discretization scheme to obtain a lumped approximation of the distributed parameter system followed by the formulation and solution of an optimal state estimation problem which involves computing sensor locations so that an appropriate functional that includes penalty on the estimation error and the measurement noise is minimized.

Significant research efforts have also been made on the integrated optimal placement of controllers and sensors for various classes of linear distributed parameter systems (see, for example, Amouroux, Di Pillo, & Grippo, 1976; Ichikawa & Ryan, 1977; Courdesses, 1978; Malandrakis, 1979; Omatu & Seinfeld, 1983 and the review paper of Kubrusly & Malebranche, 1985). Despite the progress on optimal sensor placement and the availability of results on the integration of linear feedback control with actuator placement for linear parabolic PDEs, there are no results on the integration of nonlinear output feedback control with optimal placement of control actuators and measurement sensors for transport-reaction processes described by nonlinear parabolic PDEs.

This paper proposes a general and practical methodology for the integration of nonlinear output feedback control with optimal placement of control actuators and measurement sensors for transport-reaction processes described by a broad class of quasi-linear parabolic partial differential equations (PDEs) for which the eigenspectrum of the spatial differential operator can be partitioned into a finite-dimensional slow one and an infinite-dimensional stable fast complement. Initially, Galerkin's method is employed to derive finite-dimensional approximations of the PDE system which are used for the synthesis of stabilizing nonlinear state feedback controllers via geometric techniques. The optimal actuator location problem is subsequently formulated as the one of minimizing a meaningful cost functional that includes penalty on the response of the closed-loop system and the control action and is solved by using standard unconstrained optimization techniques. Then, under the assumption that the number of measurement sensors is equal to the number of slow modes, we employ a procedure proposed in Christofides and Baker (1999) for obtaining estimates for the states of the approximate finite-dimensional model from the measurements. The estimates are combined with the state feedback controllers to derive output feedback controllers. The optimal location of the measurement sensors is computed by minimizing a cost function of the estimation error in the closed-loop infinite-dimensional system. It is rigorously established that the proposed output feedback controllers enforce stability in the closed-loop infinite-dimensional system and that the solution to the optimal actuator/sensor problem, which is obtained on the basis of the closed-loop finite-dimensional system, is near-optimal in the sense that it approaches the optimal solution for the infinite-dimensional system as the separation of the slow and fast eigenmodes increases. The proposed methodology is successfully applied to a diffusion–reaction process and a non-isothermal tubular reactor with recycle to derive nonlinear output feedback controllers and compute optimal actuator/sensor locations for stabilization of unstable steady states.

2. Preliminaries

2.1. Description of parabolic PDE systems

We consider transport-reaction processes described by quasi-linear parabolic PDE systems of the form

$$\frac{\partial \bar{x}}{\partial t} = A\frac{\partial \bar{x}}{\partial z} + B\frac{\partial^2 \bar{x}}{\partial z^2} + wb(z)u + f(\bar{x}),$$
$$y_c^i = \int_\alpha^\beta c^i(z)k\bar{x}(z,t)\,\mathrm{d}z, \quad i = 1,\ldots,l, \tag{1}$$
$$y_m^\kappa = \int_\alpha^\beta s^\kappa(z)\omega\bar{x}(z,t)\,\mathrm{d}z, \quad \kappa = 1,\ldots,p,$$

subject to the boundary conditions:

$$C_1\bar{x}(\alpha,t) + D_1\frac{\partial \bar{x}}{\partial z}(\alpha,t) = R_1,$$
$$C_2\bar{x}(\beta,t) + D_2\frac{\partial \bar{x}}{\partial z}(\beta,t) = R_2, \tag{2}$$

and the initial condition:

$$\bar{x}(z,0) = \bar{x}_0(z), \tag{3}$$

where $\bar{x}(z,t) = [\bar{x}_1(z,t) \ \cdots \ \bar{x}_n(z,t)]^{\mathrm{T}} \in \mathbb{R}^n$ denotes the vector of state variables, $z \in [\alpha,\beta] \subset \mathbb{R}$ is the spatial coordinate, $t \in [0,\infty)$ is the time, $u = [u^1 \ u^2 \ \cdots \ u^l]^{\mathrm{T}} \in \mathbb{R}^l$ denotes the vector of manipulated inputs, $y_c^i \in \mathbb{R}$ denotes the ith controlled output, and $y_m^\kappa \in \mathbb{R}$ denotes the κth measured output. $\partial\bar{x}/\partial z, \partial^2\bar{x}/\partial z^2$ denote the first- and second-order spatial derivatives of $\bar{x}$, $f(\bar{x})$ is a nonlinear vector function, $w, k\omega$ are constant vectors, A, B, C_1, D_1, C_2, D_2 are constant matrices, R_1, R_2 are column vectors, and $\bar{x}_0(z)$ is the initial condition. $b(z)$ is a known smooth vector function of z of the form $b(z) = [b^1(z) \ b^2(z) \ \cdots \ b^l(z)]$, where $b^i(z)$ describes how the control action $u^i(t)$ is distributed in the interval $[\alpha,\beta]$, $c^i(z)$ is a known smooth function of z which is determined by the desired performance specifications in the interval $[\alpha,\beta]$, and $s^\kappa(z)$ is a known smooth function of z which depends on the shape (point or distributing sensing) of the measurement sensors in the interval $[\alpha,\beta]$. Whenever the control action enters the system at a single point z_0, with $z_0 \in [\alpha,\beta]$ (i.e. point actuation), the function $b^i(z)$ is taken to be nonzero in a finite spatial interval of the form $[z_0-\varepsilon, z_0+\varepsilon]$, where ε is a small positive real number, and zero elsewhere in $[\alpha,\beta]$. Fig. 1 shows the location of the manipulated inputs, controlled outputs, and measured outputs in the case of a prototype example. Throughout the paper, we will use the order of magnitude notation $O(\varepsilon)$. In particular, $\delta(\varepsilon) = O(\varepsilon)$ if there exist positive real numbers k_1 and k_2 such that: $|\delta(\varepsilon)| \leqslant k_1|\varepsilon|, \ \forall|\varepsilon| < k_2$.

Referring to the system of Eq. (1), several remarks are in order: (a) the spatial differential operator is linear; this assumption is valid for diffusion–convection–reaction processes where the diffusion coefficient and the conductivity can be taken independent of temperature and concentrations, (b) the manipulated input enters the system in a linear and affine fashion; this is typically the case in many practical applications where, for example, the wall temperature is chosen as the manipulated input, and (c) the nonlinearities appear in an additive fashion (e.g., complex reaction rates, Arrhenius dependence of reaction rates on temperature).

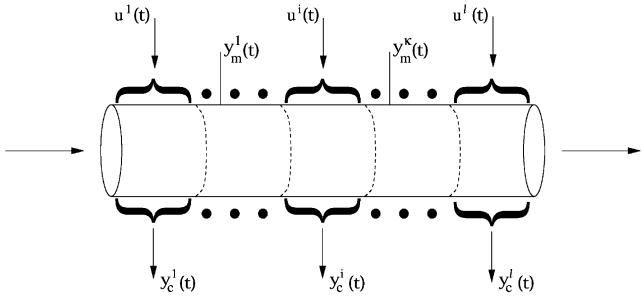

Fig. 1. Location of the manipulated inputs, controlled outputs, and measured outputs in the case of a prototype example.

In the remainder of this section, we precisely characterize the class of parabolic PDE systems of the form of Eq. (1) which we consider in the manuscript. To this end, we formulate the parabolic PDE system of Eq. (1) as an infinite-dimensional system in the Hilbert space $\mathscr{H}([\alpha,\beta];\mathbb{R}^n)$ (this will also simplify the notation of the paper, since the boundary conditions of Eq. (2) will be directly included in the formulation; see Eq. (8) below), with $\mathscr{H}$ being the space of n-dimensional vector functions defined on $[\alpha,\beta]$ that satisfy the boundary condition of Eq. (2), with inner product and norm

$$(\omega_1,\omega_2) = \int_\alpha^\beta (\omega_1(z),\omega_2(z))_{\mathbb{R}^n}\,\mathrm{d}z,$$
$$\|\omega_1\|_2 = (\omega_1,\omega_1)^{1/2}, \tag{4}$$

where ω_1, ω_2 are two elements of $\mathscr{H}([\alpha,\beta];\mathbb{R}^n)$ and the notation $(\cdot,\cdot)_{\mathbb{R}^n}$ denotes the standard inner product in $\mathbb{R}^n$. Defining the state function x on $\mathscr{H}([\alpha,\beta];\mathbb{R}^n)$ as

$$x(t) = \bar{x}(z,t), \quad t > 0, \ z \in [\alpha,\beta], \tag{5}$$

the operator $\mathscr{A}$ in $\mathscr{H}([\alpha,\beta];\mathbb{R}^n)$ as

$$\mathscr{A}x = A\frac{\partial \bar{x}}{\partial z} + B\frac{\partial^2 \bar{x}}{\partial z^2},$$
$$x \in D(\mathscr{A}) = \Big\{ x \in \mathscr{H}([\alpha,\beta];\mathbb{R}^n);$$
$$C_1\bar{x}(\alpha,t) + D_1\frac{\partial \bar{x}}{\partial z}(\alpha,t) = R_1;$$
$$C_2\bar{x}(\beta,t) + D_2\frac{\partial \bar{x}}{\partial z}(\beta,t) = R_2 \Big\}, \tag{6}$$

and the input, controlled output, and measured output operators as

$$\mathscr{B}u = wbu, \quad \mathscr{C}x = (c,kx), \quad \mathscr{S}x = (s,\omega x), \tag{7}$$

the system of Eqs. (1)–(3) takes the form

$$\dot{x} = \mathscr{A}x + \mathscr{B}u + f(x), \quad x(0) = x_0,$$
$$y_c = \mathscr{C}x, \quad y_m = \mathscr{S}x, \tag{8}$$

where $f(x(t)) = f(\bar{x}(z,t))$ and $x_0 = \bar{x}_0(z)$. We assume that the nonlinear terms $f(x)$ are locally Lipschitz with respect to their arguments and satisfy $f(0) = 0$. For $\mathscr{A}$, the eigenvalue problem is defined as

$$\mathscr{A}\phi_j = \lambda_j\phi_j, \quad j = 1, \ldots, \infty, \tag{9}$$

where λ_j denotes an eigenvalue and ϕ_j denotes an eigenfunction; the eigenspectrum of $\mathscr{A}$, $\sigma(\mathscr{A})$, is defined as the set of all eigenvalues of $\mathscr{A}$, i.e. $\sigma(\mathscr{A}) = \{\lambda_1, \lambda_2, \ldots, \}$. Assumption 1 (Christofides and Daoutidis, 1997) that follows states that the eigenspectrum of $\mathscr{A}$ can be partitioned into a finite-dimensional part consisting of m slow eigenvalues and a stable infinite-dimensional complement containing the remaining fast eigenvalues, and that the separation between the slow and fast eigenvalues of $\mathscr{A}$ is large.

Assumption 1. *(1) $Re\{\lambda_1\} \geqslant Re\{\lambda_2\} \geqslant \cdots \geqslant Re\{\lambda_j\} \geqslant \cdots$, where $Re\{\lambda_j\}$ denotes the real part of λ_j.*

(2) $\sigma(\mathscr{A})$ can be partitioned as $\sigma(\mathscr{A}) = \sigma_1(\mathscr{A}) + \sigma_2(\mathscr{A})$, where $\sigma_1(\mathscr{A})$ consists of the first m (with m finite) eigenvalues, i.e. $\sigma_1(\mathscr{A}) = \{\lambda_1, \ldots, \lambda_m\}$, and $\frac{|Re\{\lambda_1\}|}{|Re\{\lambda_m\}|} = O(1)$.

(3) $Re\lambda_{m+1} < 0$ and $\frac{|Re\ \{\lambda_m\}|}{|Re\{\lambda_{m+1}\}|} = O(\varepsilon)$ where $\varepsilon < 1$ is a small positive number.

The assumption of finite number of unstable eigenvalues is always satisfied for nonlinear parabolic PDE systems (Friedman, 1976), while the assumption of discrete eigenspectrum and the assumption of existence of only a few dominant modes that describe the dynamics of the nonlinear parabolic PDE system are usually satisfied by the majority of diffusion–convection–reaction processes (see the examples of Sections 6 and 7).

2.2. Galerkin's method

We will now review the application of standard Galerkin's method to the system of Eq. (8) to derive an approximate finite-dimensional system. Let $\mathscr{H}_s$, $\mathscr{H}_f$ be modal subspaces of $\mathscr{A}$, defined as $\mathscr{H}_s = \text{span}\{\phi_1, \phi_2, \ldots, \phi_m\}$ and $\mathscr{H}_f = \text{span}\{\phi_{m+1}, \phi_{m+2}, \ldots\}$ (the existence of $\mathscr{H}_s$, $\mathscr{H}_f$ follows from Assumption 1). Defining the orthogonal projection operators P_s and P_f such that $x_s = P_s x$, $x_f = P_f x$, the state x of the system of Eq. (8) can be decomposed as

$$x = x_s + x_f = P_s x + P_f x. \tag{10}$$

Applying P_s and P_f to the system of Eq. (8) and using the above decomposition for x, the system of Eq. (8) can be equivalently written in the following form:

$$\frac{dx_s}{dt} = \mathscr{A}_s x_s + \mathscr{B}_s u + f_s(x_s, x_f),$$
$$\frac{\partial x_f}{\partial t} = \mathscr{A}_f x_f + \mathscr{B}_f u + f_f(x_s, x_f),$$
$$y_c = \mathscr{C}x_s + \mathscr{C}x_f, \quad y_m = \mathscr{S}x_s + \mathscr{S}x_f,$$
$$x_s(0) = P_s x(0) = P_s x_0, \quad x_f(0) = P_f x(0) = P_f x_0, \tag{11}$$

where $\mathscr{A}_s = P_s\mathscr{A}P_s$, $\mathscr{B}_s = P_s\mathscr{B}$, $f_s = P_s f$, $\mathscr{A}_f = P_f\mathscr{A}P_f$, $\mathscr{B}_f = P_f\mathscr{B}$ and $f_f = P_f f$ and the notation $\partial x_f/\partial t$ is used to denote that the state x_f belongs in an infinite-dimensional space. In the above system, $\mathscr{A}_s$ is a diagonal matrix of dimension $m \times m$ of the form $\mathscr{A}_s = \text{diag}\{\lambda_j\}$, $f_s(x_s, x_f)$ and $f_f(x_s, x_f)$ are Lipschitz vector functions, and $\mathscr{A}_f$ is an unbounded differential operator which is exponentially stable (following from part (3) of Assumption 1 and the selection of $\mathscr{H}_s, \mathscr{H}_f$). Neglecting the fast and stable infinite-dimensional x_f-subsystem in the system of Eq. (11), the following m-dimensional slow system is obtained:

$$\frac{d\tilde{x}_s}{dt} = \mathscr{A}_s\tilde{x}_s + \mathscr{B}_s u + f_s(\tilde{x}_s, 0),$$
$$\tilde{y}_c = \mathscr{C}\tilde{x}_s, \quad \tilde{y}_m = \mathscr{S}\tilde{x}_s, \tag{12}$$

where the tilde symbol in $\tilde{x}_s$, $\tilde{y}_c$ and $\tilde{y}_m$ denotes that the state $\tilde{x}_s$, the controlled output $\tilde{y}_c$, and the measured output $\tilde{y}_m$ are associated with the approximation of the slow x_s-subsystem.

Remark 1. We note that the above model reduction procedure which led to the approximate ODE system of Eq. (11) can also be used, when empirical eigenfunctions of the system of Eq. (8) computed through Karhunen–Loéve expansion (see Christofides, 2001 for details) are used as basis functions in $\mathscr{H}_s$ and $\mathscr{H}_f$ instead of the eigenfunctions of $\mathscr{A}$. Furthermore, we note that due to the separation of the fast and slow modes of the spatial differential operator (which is characterized by ε; part (3) of Assumption 1), the coupling of the x_s and x_f subsystems in the interconnection of Eq. (11) through the terms $f_s(x_s, x_f)$ and $f_f(x_s, x_f)$ in a bounded region of the state space is weak (i.e., it scales with ε and disappears as $\varepsilon \to 0$); this property is the basis for using the finite-dimensional system of Eq. (12) for nonlinear output feedback controller design and optimal actuator/sensor placement.

3. Problem statement and solution framework

In this paper, we address the problem of computing optimal locations of point control actuators and point measurement sensors associated with nonlinear output

feedback control laws of the following general form:

$$u = \mathscr{F}(y_m), \tag{13}$$

where $\mathscr{F}(y_m)$ is a nonlinear vector function and y_m denotes the vector of measured outputs, so that the following properties are enforced in the closed-loop system: (a) exponential stability, and (b) the solution to the optimal actuator/sensor location problem, which is obtained on the basis of the closed-loop finite-dimensional system, is near-optimal in the sense that it approaches the optimal solution for the infinite-dimensional system as the separation of the slow and fast eigenmodes increases. To address this problem, we will initially synthesize stabilizing nonlinear state feedback controllers via geometric techniques on the basis of finite-dimensional approximations of the PDE system obtained via Galerkin's method. The optimal actuator location problem will be subsequently formulated as the one of minimizing a meaningful cost functional that includes penalty on the response of the closed-loop system and the control action and will be solved by using standard unconstrained optimization techniques. Then, under the assumption that the number of measurement sensors is equal to the number of slow modes, we will employ a procedure proposed in Christofides and Baker (1999) for obtaining estimates for the states of the approximate finite-dimensional model from the measurements. The estimates will be combined with the state feedback controllers to derive output feedback controllers. The optimal location of the measurement sensors will be computed by minimizing a cost function of the estimation error in the closed-loop infinite-dimensional system. It will be established by using singular perturbation techniques that the desired properties are enforced in the closed-loop system, provided that the separation of the slow and fast eigenmodes is sufficiently large.

4. Integrating nonlinear control and optimal actuator placement

4.1. Nonlinear state feedback controller synthesis

In this section, we assume that measurements of the states of the PDE system of Eq. (12) are available and address the problem of synthesizing nonlinear static state feedback control laws of the general form

$$u = \mathscr{F}(z_a, \tilde{x}_s), \tag{14}$$

where $\mathscr{F}(z_a, \tilde{x}_s)$ is a nonlinear vector function and z_a denotes the vector of the actuator locations, that guarantee exponential stability of the closed-loop finite-dimensional system. To this end, we will need the following assumption (see Remark 3 below for a discussion on this assumption).

Assumption 2. *$l = m$ (i.e., the number of control actuators is equal to the number of slow modes), and the inverse of the matrix $\mathscr{B}_s$ exists.*

Proposition 1 that follows provides the explicit formula for the state feedback controller that achieves the control objective.

Proposition 1. *Consider the finite-dimensional system of Eq.* (12) *for which Assumption* 2 *holds. Then, the state feedback controller*:

$$u = \mathscr{B}_s^{-1}((\Lambda_s - \mathscr{A}_s)\tilde{x}_s - f_s(\tilde{x}_s, 0)), \tag{15}$$

where Λ_s is a stable matrix, guarantees global exponential stability of the closed-loop finite-dimensional system.

Remark 2. The structure of the closed-loop finite-dimensional system under the controller of Eq. (15) has the following form:

$$\dot{\tilde{x}}_s = \Lambda_s \tilde{x}_s, \tag{16}$$

and thus, the response of this system depends only on the stable matrix Λ_s and the initial condition, $x_s(0)$, and is independent of the actuator locations.

Remark 3. The requirement $l = m$ is sufficient and not necessary, and it is made to simplify the solution of the controller synthesis problem. Full linearization of the closed-loop finite-dimensional system through coordinate change and nonlinear feedback can be achieved for any number of manipulated inputs (i.e., for any $l \in [1, m]$), provided that an appropriate set of involutivity conditions is satisfied by the corresponding vector fields of the system of Eq. (12) (see Isidori, 1989 for details).

4.2. Computation of optimal location of control actuators

In this subsection, we compute the actuator locations so that the state feedback controller of Eq. (15) is near-optimal for the full PDE system of Eq. (11) with respect to a meaningful cost functional which is defined over the infinite time-interval and imposes penalty on the response of the closed-loop system and the control action. To this end, we initially focus on the ODE system of Eq. (12) and consider the following cost functional:

$$J_s = \int_0^\infty ((\tilde{x}_s^{\mathrm{T}}(x_s(0), t), Q_s \tilde{x}_s(x_s(0), t)) + u^{\mathrm{T}}(\tilde{x}_s(x_s(0), t), z_a) R u(\tilde{x}_s(x_s(0), t), z_a)) \, \mathrm{d}t, \tag{17}$$

where Q_s and R are positive definite matrices. The cost of Eq. (17) is well defined and meaningful since it imposes penalty on the response of the closed-loop

finite-dimensional system and the control action. However, a potential problem of this cost is its dependence on the choice of a particular initial condition, $x_s(0)$, and thus, the solution to the optimal placement problem based on this cost may lead to actuator locations that perform very poorly for a large set of initial conditions. To eliminate this dependence and obtain optimality over a broad set of initial conditions, we follow Levine and Athans (1978) and consider an average cost over a set of m linearly independent initial conditions, $x_s^i(0)$, $i=1,\ldots,m$, of the following form:

$$\hat{J}_s = \frac{1}{m}\sum_{i=1}^{m}\int_0^\infty ((\tilde{x}_s^{\mathrm{T}}(x_s^i(0),t), Q_s\tilde{x}_s(x_s^i(0),t)) + u^{\mathrm{T}}(\tilde{x}_s(x_s^i(0),t),z_a)Ru(\tilde{x}_s(x_s^i(0),t),z_a))\,\mathrm{d}t. \quad (18)$$

Referring to the above cost, we first note that the penalty on the response of the closed-loop system

$$\hat{J}_{xs} = \frac{1}{m}\sum_{i=1}^{m}\int_0^\infty (\tilde{x}_s^{\mathrm{T}}(x_s^i(0),t), Q_s\tilde{x}_s(x_s^i(0),t))\,\mathrm{d}t \quad (19)$$

is finite because the solution of the closed-loop system of Eq. (16) is exponentially stable by appropriate choice of Λ_s. Moreover, $\hat{J}_{xs}$ is independent of the actuator locations (Remark 2), and thus, the optimal actuator placement problem reduces to the one of minimizing the following cost which only includes penalty on the control action:

$$\hat{J}_{us} = \frac{1}{m}\sum_{i=1}^{m}\int_0^\infty u^{\mathrm{T}}(\tilde{x}_s(x_s^i(0),t),z_a)Ru(\tilde{x}_s(x_s^i(0),t),z_a)\,\mathrm{d}t$$

$\hat{J}_{us}$ is a function of multiple variables, $z_a = [z_{a1}\ z_{a2}\ \cdots\ z_{al}]$, and thus, it obtains its local minimum values when its gradient with respect to the actuator locations is equal to zero, i.e.:

$$\frac{\partial \hat{J}_{us}}{\partial z_a} = \left[\frac{\partial \hat{J}_{us}}{\partial z_{a1}}\ \cdots\ \frac{\partial \hat{J}_{us}}{\partial z_{al}}\right]^{\mathrm{T}} = [0\ \cdots\ 0]^{\mathrm{T}}, \quad (20)$$

and $\nabla_{z_a z_a}\hat{J}_{us}(z_{am}) > 0$ where $\nabla_{z_a z_a}\hat{J}_{us}$ is the Hessian matrix of $\hat{J}_{us}$ and z_{am} is a solution of the system of nonlinear algebraic equations of Eq. (20) (which includes l equations with l unknowns). The solution z_{am} for which the above conditions are satisfied and $\hat{J}_{us}$ obtains its smallest value (global minimum) corresponds to the optimal actuator locations for the closed-loop finite-dimensional system. Theorem 1 that follows establishes that these locations are near-optimal for the closed-loop infinite-dimensional system (the proof of this theorem can be found in the Appendix).

Theorem 1. *Consider the infinite-dimensional system of Eq.* (11) *for which Assumption* 1 *holds, and the finite-dimensional system of Eq.* (12), *for which Assumption* 2 *holds. Then, there exist positive real numbers* μ_1, μ_2 *and* ε^* *such that if* $|x_s(0)| \leqslant \mu_1$, $\|x_f(0)\|_2 \leqslant \mu_2$, *and* $\varepsilon \in (0, \varepsilon^*]$, *then the controller of Eq.* (13): (a) *guarantees exponential stability of the closed-loop infinite-dimensional system, and*

(b) *the optimal locations of the point actuators obtained for the closed-loop finite-dimensional system are near-optimal for the closed-loop infinite-dimensional system in the sense that*:

$$\hat{J} = \frac{1}{m}\sum_{i=1}^{m}\int_0^\infty ((x_s^{\mathrm{T}}(x_s^i(0),t), Q_s x_s(x_s^i(0),t)) + (x_f^{\mathrm{T}}(x_s^i(0),t), Q_f x_f(x_f^i(0),t)) + u^{\mathrm{T}}(x_s(x_s^i(0),t),z_a)Ru(x_s(x_s^i(0),t),z_a))\,\mathrm{d}t \to \hat{J}_s \quad \text{as } \varepsilon \to 0, \quad (21)$$

where Q_f *is an unbounded positive definite operator and* $\hat{J}$ *is the average cost function associated with the controller of Eq.* (15) *and the infinite-dimensional system of Eq.* (11).

Remark 4. Note that even though the response of the closed-loop finite-dimensional system of Eq. (16) is independent of the actuator locations, the response of the closed-loop infinite-dimensional system does depend on the actuators locations. However, this dependence is scaled by ε, and therefore, it decreases as we increase the number of modes included in the finite-dimensional system used for controller design.

Remark 5. In general, the solution to the system of Eq. (20) can be computed through combination of numerical integration techniques and multivariable Newton's method.

Remark 6. The results of this section, state feedback control and optimal actuator placement, can be generalized to the case where the finite-dimensional approximation of the system of Eq. (11) is obtained through combination of Galerkin's method with approximate inertial manifolds (Christofides, 2001). This would lead to a higher than $O(\varepsilon)$ closeness between the solution of the finite-dimensional closed-loop system and the solution of the infinite-dimensional closed-loop system (see Christofides (2001) for a detailed study of this issue), which, in turn, would allow to obtain a better characterization and a significant improvement of the closed-loop infinite-dimensional system performance. However, since the objective of the present work is output feedback control with optimal actuator/sensor placement, we do not pursue this approach because the error that will be introduced in the estimates of the slow states from the output measurements will be of $O(\varepsilon)$ (see Assumption 3 below), and thus, it is not possible to obtain a better than $O(\varepsilon)$ characterization of the closed-loop infinite-dimensional

system performance under the static output feedback controller presented in the next section.

5. Integrating nonlinear output feedback control and optimal actuator/sensor placement

The nonlinear controller of Eq. (15) was derived under the assumption that measurements of the state variables, $\bar{x}(z,t)$, are available at all positions and times. However, from a practical point of view, measurements of the state variables are only available at a finite number of spatial positions, while in addition, there are many applications where measurements of process state variables cannot be obtained on-line (for example, concentrations of certain species in a chemical reactor may not be measured on-line). Motivated by these practical problems, we address in this section: (a) the synthesis of nonlinear output feedback controllers that use measurements of the process outputs, y_m, to enforce stability in the closed-loop infinite-dimensional system, and (b) the computation of optimal locations of the measurement sensors. Specifically, we consider output feedback control laws of the general form

$$u(t) = \mathscr{F}(y_m), \tag{22}$$

where $\mathscr{F}(y_m)$ is a nonlinear vector function and y_m is the vector of measured outputs. The synthesis of the controller of Eq. (22) will be achieved by combining the state feedback controller of Eq. (15) with a procedure proposed in Christofides and Baker (1999) for obtaining estimates for the states of the approximate ODE model of Eq. (12) from the measurements. To this end, we need to impose the following requirement on the number of measured outputs in order to obtain estimates of the states x_s of the finite-dimensional system of Eq. (12), from the measurements y_m^κ, $\kappa = 1, \ldots, p$.

Assumption 3. *$p=m$ (i.e., the number of measurements is equal to the number of slow modes), and the inverse of the operator $\mathscr{S}$ exist, so that $\hat{x}_s = \mathscr{S}^{-1} y_m$.*

We note that the requirement that the inverse of the operator S exists can be achieved by appropriate choice of the location of the measurement sensors (i.e., functions $s^\kappa(z)$). The optimal locations for the measurement sensors can be computed by minimizing an average cost function of the estimation error of the closed-loop infinite-dimensional system of the form

$$\hat{J}(e) = \frac{1}{m}\sum_{i=1}^{m}\int_0^\infty (\|x_s(x_s^i(0),t) - \hat{x}_s(x_s^i(0),t)\|_2)\,\mathrm{d}t, \tag{23}$$

where x_s is the slow state of the closed-loop infinite-dimensional system of Eq. (11), $\hat{x}_s = \mathscr{S}^{-1} y_m$, and $e(t) = \|x_s - \hat{x}_s\|_2$ is the estimation error. In contrast to the solution of the optimal location problem for the control actuators, the solution to this optimization problem requires the solution of the closed-loop infinite-dimensional system in order to compute x_s, and $\hat{x}_s$ (from the measurements y_m^κ, $\kappa = 1, 2, \ldots, p$), and thus, it is more computationally demanding.

Theorem 2 that follows establishes that the proposed output feedback controller enforces stability in the closed-loop infinite-dimensional system and that the solution to the optimal actuator/sensor problem, which is obtained on the basis of the closed-loop finite-dimensional system, is near-optimal in the sense that it approaches the optimal solution for the infinite-dimensional system as the separation of the slow and fast eigenmodes increases. The proof of this theorem can be found in the Appendix.

Theorem 2. *Consider the full system of Eq. (11) for which Assumption 1 holds, and the finite-dimensional system of Eq. (12), for which Assumptions 2 and 3 hold, under the nonlinear output feedback controller*:

$$\begin{aligned} &\hat{x}_s = \mathscr{S}^{-1} y_m, \\ &u = \mathscr{B}_s^{-1}((\Lambda_s - \mathscr{A}_s)\hat{x}_s - f_s(\hat{x}_s, 0)). \end{aligned} \tag{24}$$

Then, there exist positive real numbers μ_1, μ_2 and ε^* such that if $|x_s(0)| \leqslant \mu_1$, $\|x_f(0)\|_2 \leqslant \mu_2$, and $\varepsilon \in (0, \varepsilon^*]$, then the controller of Eq. (24):

(a) *guarantees exponential stability of the closed-loop system, and*
(b) *the locations of the point actuators and measurement sensors are near-optimal in the sense that the cost function associated with the controller of Eq. (24) and the system of Eq. (11) satisfies*

$$\begin{aligned} \hat{J} = \frac{1}{m}\sum_{i=1}^{m}\int_0^\infty &((x_s^{\mathrm{T}}(x_s^i(0),t), Q_s x_s(x_s^i(0),t)) \\ &+ (x_f^{\mathrm{T}}(x_s^i(0),t), Q_f x_f(x_f^i(0),t)) \\ &+ u^{\mathrm{T}}(x_s(x_s^i(0)),t,z_a) R u(x_s(x_s^i(0)),t,z_a))\,\mathrm{d}t \to \hat{J}_s \\ &\text{as } \varepsilon \to 0, \end{aligned} \tag{25}$$

where $\hat{J}$ and $\hat{J}_s$ are the average cost functions of the infinite-dimensional system of Eq. (11) and the finite-dimensional system of Eq. (12), respectively, under the output feedback controller of Eq. (24).

Remark 7. We note that the controller of Eq. (24) uses static feedback of the measured outputs y_m^κ, $\kappa = 1, \ldots, p$, and thus, it feeds back both x_s and x_f (this is in contrast to the state feedback controller of Eq. (15) which only uses feedback of the slow state x_s). However, even though the use of x_f feedback could lead to destabilization of the stable fast subsystem, the large separation of the slow

and fast modes of the spatial differential operator (i.e., assumption that ε is sufficiently small) and the fact that the controller does not include terms of the form $O(1/\varepsilon)$ do not allow such a destabilization to occur.

In the remainder of the paper, we show two applications of the proposed approach for optimal actuator/sensor placement to a typical diffusion–reaction process and a nonisothermal tubular reactor with recycle.

6. Application to a diffusion–reaction process

6.1. Process description—control problem formulation

Consider a long, thin rod in a reactor (Fig. 2). The reactor is fed with pure species A and a zeroth order exothermic catalytic reaction of the form $A \rightarrow B$ takes place on the rod. Since the reaction is exothermic, a cooling medium which is in contact with the rod is used for cooling. Under the assumptions of constant density and heat capacity of the rod, constant conductivity of the rod, and constant temperature at both ends of the rod, the mathematical model which describes the spatiotemporal evolution of the dimensionless rod temperature consists of the following parabolic PDE:

$$\frac{\partial \bar{x}}{\partial t} = \frac{\partial^2 \bar{x}}{\partial z^2} + \beta_T e^{-\gamma/(1+\bar{x})} + \beta_U(b(z)u(t) - \bar{x}) - \beta_T e^{-\gamma}, \tag{26}$$

subject to the Dirichlet boundary conditions:

$$\bar{x}(0,t) = 0, \quad \bar{x}(\pi,t) = 0 \tag{27}$$

and the initial condition:

$$\bar{x}(z,0) = \bar{x}_0(z), \tag{28}$$

where $\bar{x}$ denotes the dimensionless temperature in the reactor, β_T denotes a dimensionless heat of reaction, γ denotes a dimensionless activation energy, β_U denotes a dimensionless heat transfer coefficient, and u denotes the manipulated input (temperature of the cooling medium). The following typical values were given to the process parameters:

$$\beta_T = 50.0, \quad \beta_U = 2.0, \quad \gamma = 4.0. \tag{29}$$

For the above values, the operating steady state $\bar{x}(z,t)=0$ is an unstable one (Fig. 3 shows the profile of evolution of open-loop rod temperature starting from initial conditions close to the steady state $\bar{x}(z,t) = 0$; the process moves to another stable steady state characterized by a maximum in the temperature profile, *hot-spot*, in the middle of the rod). A 30th order Galerkin truncation of the system of Eqs. (26)–(28) was used in our simulations in order to accurately describe the process (further increase on the order of the Galerkin truncation was found to give negligible improvement on the accuracy of the results). The control objective is to stabilize the rod temperature profile at the unstable steady state $\bar{x}(z,t) = 0$. The eigenvalue problem for the spatial differential operator of the process:

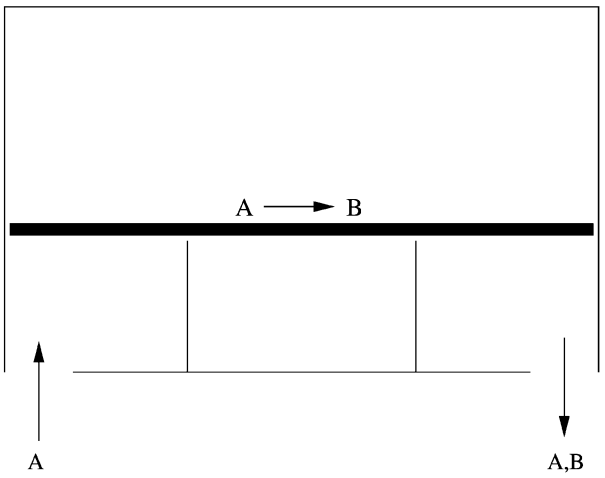

Fig. 2. Catalytic rod.

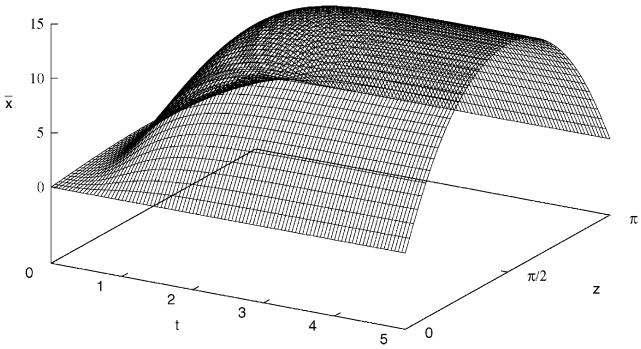

Fig. 3. Profile of evolution of rod temperature in the open-loop system.

$$\begin{aligned} &\mathscr{A}x = \frac{\partial^2 \bar{x}}{\partial z^2}, \\ &x \in D(\mathscr{A}) = \{x \in \mathscr{H}([0,\pi];\mathbb{R}); \\ &\bar{x}(0,t) = 0, \bar{x}(\pi,t) = 0\} \end{aligned} \tag{30}$$

can be solved analytically and its solution is of the form

$$\lambda_j = -j^2, \quad \phi_j(z) = \bar{\phi}_j(z) = \sqrt{\frac{2}{\pi}}\sin(j\,z), \quad j = 1,\ldots,\infty, \tag{31}$$

where $\lambda_j, \phi_j, \bar{\phi}_j$, denote the eigenvalues, eigenfunctions and adjoint eigenfunctions of $\mathscr{A}_i$, respectively. In the remainder of this section, we use the proposed method to compute the optimal locations in the case of using two and three control actuators and measurement sensors.

6.2. Two actuator/sensor example

Initially, we assume that two point control actuators and measurement sensors are used to stabilize the system. Therefore, following Assumptions 2 and 3, we use Galerkin's method to derive a second order ODE approximation of the PDE of Eq. (26) which is used for controller design and optimal actuator/sensor placement. The form of the approximate ODE system is given below:

$$\begin{bmatrix} \dot{\tilde{x}}_{s1} \\ \dot{\tilde{x}}_{s2} \end{bmatrix} = \begin{bmatrix} \lambda_1 - \beta_U & 0 \\ 0 & \lambda_2 - \beta_U \end{bmatrix} \begin{bmatrix} \tilde{x}_{s1} \\ \tilde{x}_{s2} \end{bmatrix} + \beta_U \begin{bmatrix} \bar{\phi}_1(z_{a1}) & \bar{\phi}_1(z_{a2}) \\ \bar{\phi}_2(z_{a1}) & \bar{\phi}_2(z_{a2}) \end{bmatrix} \begin{bmatrix} u_1 \\ u_2 \end{bmatrix} + \beta_T \begin{bmatrix} f_1(\tilde{x}_s, 0) \\ f_2(\tilde{x}_s, 0) \end{bmatrix}, \tag{32}$$

where z_{a1} and z_{a2} are the locations of the two point actuators and the explicit forms of the terms $f_1(\tilde{x}_s, 0)$ and $f_2(\tilde{x}_s, 0)$ are omitted for brevity. The measured output $y_m(t) \in \mathbb{R}^2$ is defined as:

$$\begin{bmatrix} y_{m1} \\ y_{m2} \end{bmatrix} = \begin{bmatrix} x(z_{s1}, t) \\ x(z_{s2}, t) \end{bmatrix}, \tag{33}$$

where z_{s1} and z_{s2} are the locations of the two point sensors. For the system of Eq. (32), the nonlinear state feedback controller of Eq. (15) takes the form

$$u = \begin{bmatrix} u_1 \\ u_2 \end{bmatrix} = B^{-1}(z_a) F(\tilde{x}_s) = \frac{1}{\beta_U} \begin{bmatrix} \bar{\phi}_1(z_{a1}) & \bar{\phi}_1(z_{a2}) \\ \bar{\phi}_2(z_{a1}) & \bar{\phi}_2(z_{a2}) \end{bmatrix}^{-1} \times \left(\begin{bmatrix} -\alpha - \lambda_1 + \beta_U & 0 \\ 0 & -\beta - \lambda_2 + \beta_U \end{bmatrix} \begin{bmatrix} (\tilde{x}_{s1}, \phi_1) \\ (\tilde{x}_{s2}, \phi_2) \end{bmatrix} + \beta_T \begin{bmatrix} (f_1(\tilde{x}_s, 0), \phi_1) \\ (f_2(\tilde{x}_s, 0), \phi_2) \end{bmatrix} \right). \tag{34}$$

Substituting the above controller into the system of Eq. (32), we obtain the following closed-loop ODE system:

$$\begin{bmatrix} \dot{\tilde{x}}_{s1} \\ \dot{\tilde{x}}_{s2} \end{bmatrix} = \begin{bmatrix} -\alpha & 0 \\ 0 & -\beta \end{bmatrix} \begin{bmatrix} \tilde{x}_{s1} \\ \tilde{x}_{s2} \end{bmatrix}, \tag{35}$$

where α and β are positive real numbers. Since the response of the above system depends only on the parameters α, β and the initial condition x_s, and is independent of the actuator locations,we compute the optimal actuator locations by minimizing the following cost functional, which only includes penalty on the control action:

$$\hat{J}_{us} = \frac{1}{2} \sum_{i=1}^{2} \int_0^\infty F^{\mathrm{T}}(\tilde{x}_s(x_s^i(0), t))(B^{-1}(z_a))^{\mathrm{T}} R B^{-1}(z_a) \times F(\tilde{x}_s(x_s^i(0), t))\, \mathrm{d}t. \tag{36}$$

Table 1
Results for two control actuators

Case	Actuator locations	$\hat{J}_u$	$\hat{J}_x$	$\hat{J}$
Optimal	$0.39\pi, 0.66\pi$	0.8075	0.5332	1.3407
Linearized	$0.32\pi, 0.68\pi$	0.8980	0.5414	1.4416
3	$0.20\pi, 0.80\pi$	5.2109	1.7957	7.0066
4	$0.30\pi, 0.70\pi$	0.9065	0.5608	1.5473

Using the following values for the parameters $\alpha = \beta = 1$, $x_s^1(0) = \phi_1$, and $x_s^2(0) = \phi_2$, and taking R, Q_s, Q_f to be unit matrices of appropriate dimensions, the optimal actuator locations were found to be: $z_{a1} = 0.39\pi$ and $z_{a2} = 0.66\pi$.

Finally, we compute the optimal sensor locations by minimizing the following cost functional of the estimation error:

$$\hat{J}(e) = \frac{1}{2} \sum_{i=1}^{2} \int_0^\infty (\|x_s(x_s^i(0)) - \hat{x}_s(x_s^i(0))\|_2))\, \mathrm{d}t, \tag{37}$$

where x_s is obtained from the simulation of the full-order closed-loop system of Eq. (11), and $\hat{x}_s$ is obtained from the measured outputs of the full-order closed-loop system as shown below:

$$\begin{bmatrix} \hat{x}_{s1} \\ \hat{x}_{s2} \end{bmatrix} = \begin{bmatrix} \phi_1(z_{s1}) & \phi_2(z_{s1}) \\ \phi_1(z_{s2}) & \phi_2(z_{s2}) \end{bmatrix}^{-1} \begin{bmatrix} y_{m1}(z_{s1}, t) \\ y_{m2}(z_{s2}, t) \end{bmatrix}. \tag{38}$$

We found the optimal location of measurement sensors to be: $z_{s1} = 0.31\pi$ and $z_{s2} = 0.72\pi$. Finally, by combining the state feedback controller of Eq. (34) with the measurements, and the optimal actuator/sensor locations, we derive the following nonlinear output feedback controller:

$$\begin{bmatrix} \hat{x}_{s1} \\ \hat{x}_{s2} \end{bmatrix} = \begin{bmatrix} \phi_1(z_{s1}) & \phi_2(z_{s1}) \\ \phi_1(z_{s2}) & \phi_2(z_{s2}) \end{bmatrix}^{-1} \begin{bmatrix} y_{m1}(z_{s1}, t) \\ y_{m2}(z_{s2}, t) \end{bmatrix}$$

$$u = \frac{1}{\beta_U} \begin{bmatrix} \bar{\phi}_1(z_{a1}) & \bar{\phi}_1(z_{a2}) \\ \bar{\phi}_2(z_{a1}) & \bar{\phi}_2(z_{a2}) \end{bmatrix}^{-1} \times \left(\begin{bmatrix} -\alpha - \lambda_1 + \beta_U & 0 \\ 0 & -\beta - \lambda_2 + \beta_U \end{bmatrix} \begin{bmatrix} (\hat{x}_{s1}, \phi_1) \\ (\hat{x}_{s2}, \phi_2) \end{bmatrix} + \beta_T \begin{bmatrix} (f_1(\hat{x}_s, 0), \phi_1) \\ (f_2(\hat{x}_s, 0), \phi_2) \end{bmatrix} \right). \tag{39}$$

We performed several simulation runs to evaluate the performance of the proposed method for computing optimal locations of control actuators and measurement sensors. We initially apply the state feedback controller of Eq. (34) to the 30th order Galerkin truncation of the system of Eqs. (26)–(28) and investigate the influence of the different actuator locations on the various cost functions. Table 1 shows the values of the costs $\hat{J}_u, \hat{J}_x$, and $\hat{J}$ of the full-order closed-loop system under the state feedback controller of Eq. (34), in the case of optimal actuator placement, and for the sake of comparison, the values of these costs in the case of alternative actuator placements including optimal actuator placement based on the linearized system (second line). The cost for the control

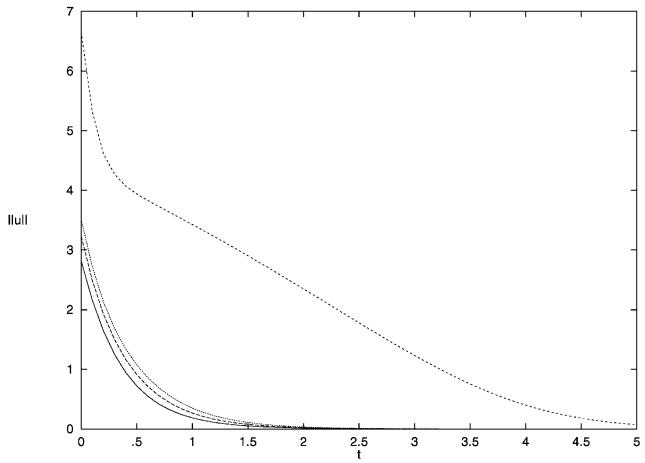

Fig. 4. Closed-loop norm of the control effort, $\|u\|$, for the two actuator/sensor example, for $x_s(0) = \phi_1$, for the optimal case (solid line), the linearized case (long-dashed line), case 3 (short-dashed line), and case 4 (dotted line).

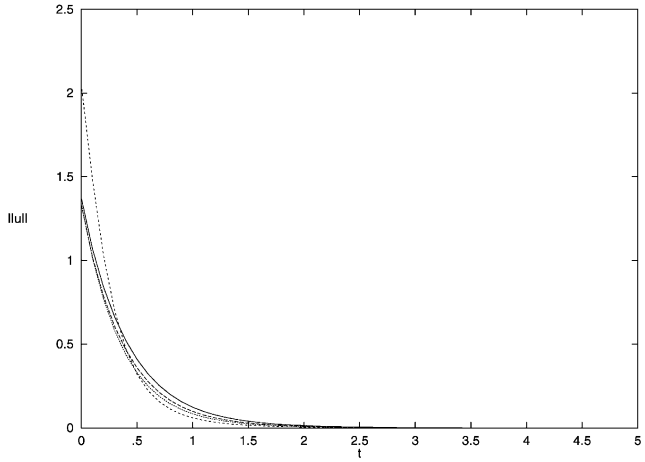

Fig. 5. Closed-loop norm of the control effort, $\|u\|$, for the two actuator/sensor example, for $x_s(0) = \phi_2$, for the optimal case (solid line), the linearized case (long-dashed line), case 3 (short-dashed line), and case 4 (dotted line).

action used to stabilize the system at $\bar{x}(z,t) = 0$ when the actuators are optimally placed, is clearly smaller than the case of actuator placement based on the linearized system (by 10.1%), case 3 (by 84.5%), and case 4 (by 10.3%). Figs. 4 and 5 show the norm of the control action, $\|u\|$, for $x(0) = \phi_1$ (Fig. 4) and $x(0) = \phi_2$ (Fig. 5), for the optimal case (solid line), the linearized case (long-dashed line), case 3 (short-dashed line), and case 4 (dotted line). Clearly, the control action used for stabilization in the case of optimal actuator placement is smaller than all the other cases.

We also tested the proposed optimal sensor locations $z_{s1} = 0.31\pi$ and $z_{s2} = 0.72\pi$. To this end, we implement the nonlinear output feedback controller of Eq. (39) on the 30th order Galerkin truncation of the system of Eqs. (26)–(28) with actuator locations $z_{a1} = 0.39\pi$ and $z_{a2} = 0.66\pi$ and different sensor locations. Table 2 shows the values of the costs $\hat{J}(e), \hat{J}_u, \hat{J}_x$, and $\hat{J}$ of the full-order closed-loop system under the output feedback controller of Eq. (39), in the case of optimal sensor placement, and for the sake of comparison, the values of these costs in the case of two other sensor locations. The estimation error of the sensor locations of 0.31π and 0.72π computed by the proposed approach is clearly smaller than the other two cases. In Fig. 6, we display the closed-loop norm of the estimation error versus time, for the optimal actuator/sensor locations, for $x_s(0) = \phi_1$ (solid line) and $x_s(0) = \phi_2$ (dashed line). We can see that for both initial conditions the estimation error is very small. Finally, Figs. 7 and 8 show the profiles of the evolution of the temperature of the rod, under output feedback control, for the optimal actuator/sensor locations, for $x_s(0) = \phi_1$ (Fig. 7), and for $x_s(0) = \phi_2$ (Fig. 8). We can see that the proposed controller with optimal actuator/sensor locations, stabilizes the system to the spatially uniform operating steady state very quickly, for both cases.

Table 2
Results for two control actuators and measurement sensors

Case	Sensor locations	$\hat{J}(e)$	$\hat{J}_u$	$\hat{J}_x$	$\hat{J}$
Optimal	$0.31\pi, 0.72\pi$	5.947e−4	0.7998	0.5150	1.3149
2	$0.48\pi, 0.71\pi$	1.613e−3	0.8384	0.5720	1.4104
3	$0.31\pi, 0.49\pi$	3.604e−3	0.8579	0.5963	1.4542

6.3. Three actuator/sensor example

In the second set of the simulation runs, we assume that three control actuators and measurement sensors are available for stabilization. Following Assumption 2, we use Galerkin's method to derive a third-order approximation of the PDE system which is used for controller design and optimal actuator/sensor placement. To reduce the size of the paper, we proceed with the presentation of the results.

Initially, we synthesized and implemented a state feedback controller on the 30th order Galerkin truncation of the system of Eqs. (26)–(28) in order to compute the optimal actuator locations. Table 3 shows the values of the costs $\hat{J}_u, \hat{J}_x$, and $\hat{J}$ of the full-order closed-loop system under state feedback control, in the case of optimal actuator placement, and for the sake of comparison, the values of these costs in the case of alternative actuator placements. Clearly, in the case of optimal actuator placement at $0.17\pi, 0.50\pi$, and 0.81π, the cost of the control action used to stabilize the system at $\bar{x}(z,t) = 0$ is smaller than case 2 (by 32.9%), and case 3 (by 66.5%). Figs. 9–11 show the norm of the control action, $\|u\|$, for $x(0) = \phi_1$ (Fig. 9), $x(0) = \phi_2$ (Fig. 10), and $x(0) = \phi_3$ (Fig. 11), for the optimal case (solid line), case 2 (long-dashed line),

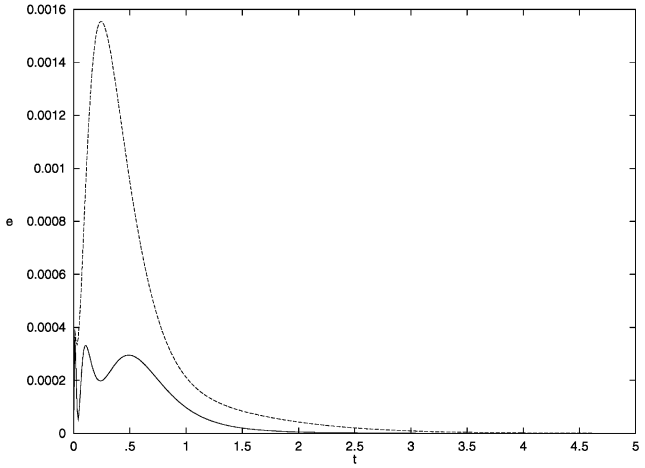

Fig. 6. Closed-loop norm of the estimation error $\|e\|$ versus time, for the two actuator/sensor example, and for the optimal actuator/sensor locations, for $x_s(0) = \phi_1$ (solid line) and $x_s(0) = \phi_2$ (dashed line).

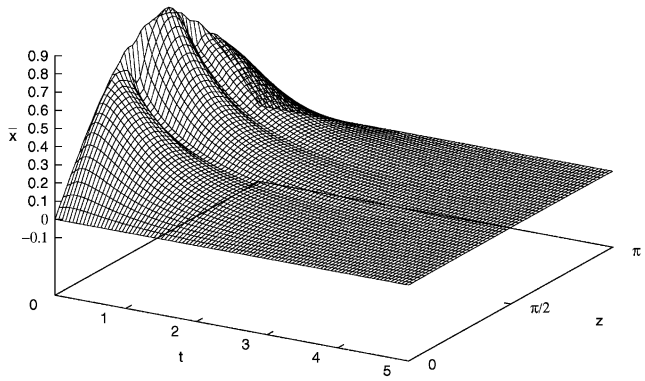

Fig. 7. Profile of evolution of the temperature of the rod, for the two actuator/sensor example, under output feedback control, for the optimal actuator/sensor locations, for $x_s(0) = \phi_1$.

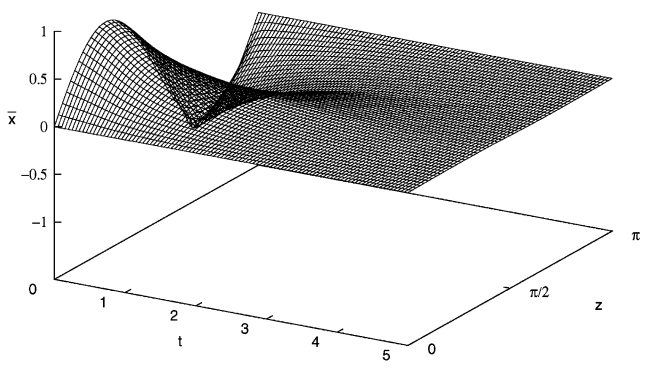

Fig. 8. Profile of evolution of the temperature of the rod, for the two actuator/sensor example, under output feedback control, for the optimal actuator/sensor locations, for $x_s(0) = \phi_2$.

Table 3
Results for three control actuators

Case	Actuator locations	$\hat{J}_u$	$\hat{J}_x$	$\hat{J}$
Optimal	$0.17\pi, 0.50\pi, 0.81\pi$	1.365	0.506	1.871
2	$0.10\pi, 0.50\pi, 0.90\pi$	2.034	0.557	2.591
3	$0.20\pi, 0.60\pi, 0.90\pi$	4.072	0.804	4.876

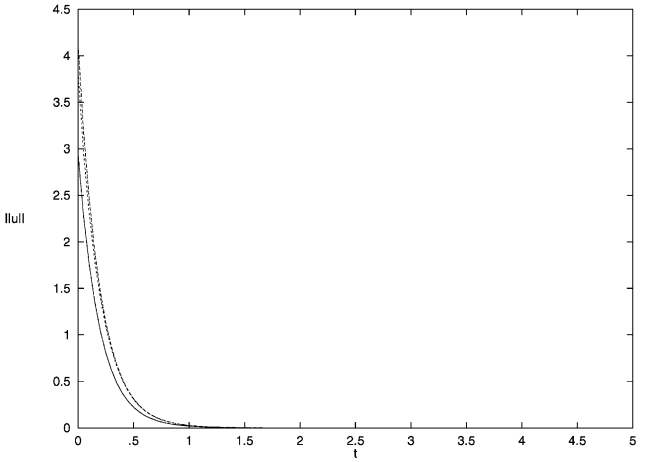

Fig. 9. Closed-loop norm of the control effort, $\|u\|$, for the three actuator/sensor example, for $x_s(0) = \phi_1$, for the optimal case (solid line), the case 2 (long-dashed line), case 3 (short-dashed line), and case 4 (dotted line).

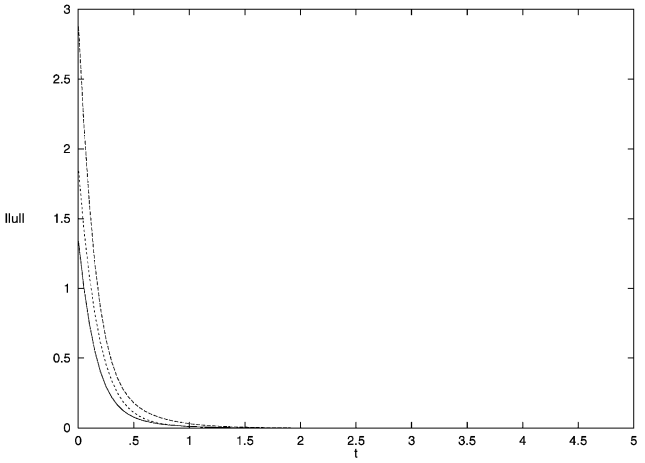

Fig. 10. Closed-loop norm of the control effort, $\|u\|$, for the three actuator/sensor example, for $x_s(0) = \phi_2$, for the optimal case (solid line), the case 2 (long-dashed line), case 3 (short-dashed line), and case 4 (dotted line).

and case 3 (short-dashed line). In the case of optimal actuator placement, the control action spent is smaller.

Subsequently, we synthesized and implemented a nonlinear output feedback controller on the 30th order Galerkin truncation of the system of Eqs. (26)–(28) with actuator locations $z_{a1} = 0.17\pi$, $z_{a2} = 0.50\pi$ and $z_{a3} = 0.81\pi$ and computed the optimal sensor locations. Table 4 shows the values of the costs $\hat{J}(e)$, $\hat{J}_u$, $\hat{J}_x$, and

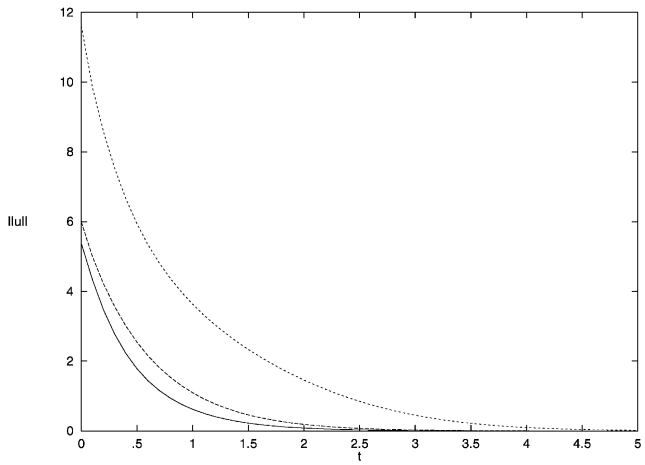

Fig. 11. Closed-loop norm of the control effort, $\|u\|$, for the three actuator/sensor example, for $x_s(0) = \phi_3$, for the optimal case (solid line), the case 2 (long-dashed line), and case 3 (short-dashed line).

Table 4
Results for three control actuators and measurement sensors

Case	Location of sensors	$\hat{J}(e)$	$\hat{J}_u$	$\hat{J}_x$	$\hat{J}$
Optimal	$0.13\pi, 0.40\pi, 0.73\pi$	3.590e−6	1.532	0.421	1.953
2	$0.13\pi, 0.43\pi, 0.74\pi$	4.730e−6	1.552	0.431	1.983
3	$0.13\pi, 0.42\pi, 0.72\pi$	7.435e−6	1.588	0.446	2.043

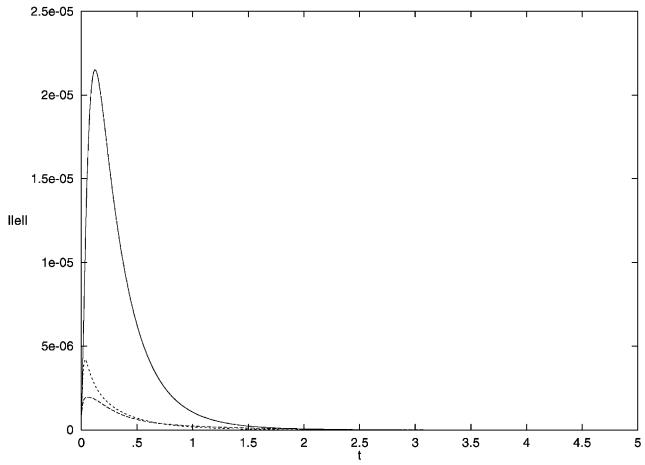

Fig. 12. Closed-loop norm of the estimation error $\|e\|$ versus time, for the three actuator/sensor example, and for the optimal actuator/sensor locations, for $x_s(0) = \phi_1$ (solid line), $x_s(0) = \phi_1$ (long-dashed line) and $x_s(0) = \phi_3$ (short-dashed line).

$\hat{J}$ of the full-order closed-loop system under output feedback control, in the case of optimal sensor placement, and for the sake of comparison, the values of these costs in the case of two other sensor locations. The estimation error of the proposed sensor locations at $0.13\pi, 0.40\pi$, and 0.73π, is clearly smaller than the other two cases. Fig. 12 shows the closed-loop norm of the estimation error versus time, for the optimal actuator/sensor locations, for $x_s(0) = \phi_1$ (solid line), for $x_s(0) = \phi_2$ (dashed line), and for $x_s(0) = \phi_3$ (dotted line). We can see that for all three initial conditions the estimation error is very small. Finally, Figs. 13–15 display the profiles of the evolution of the temperature of the rod, under output feedback control, for the optimal actuator/sensor locations, for $x_s(0) = \phi_1$ (Fig. 13), for $x_s(0) = \phi_2$ (Fig. 14),

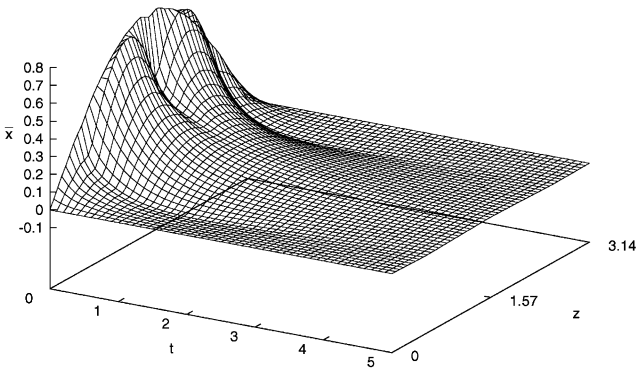

Fig. 13. Profile of evolution of the temperature of the rod, for the three actuator/sensor example, under output feedback control, for the optimal actuator/sensor locations, for $x_s(0) = \phi_1$.

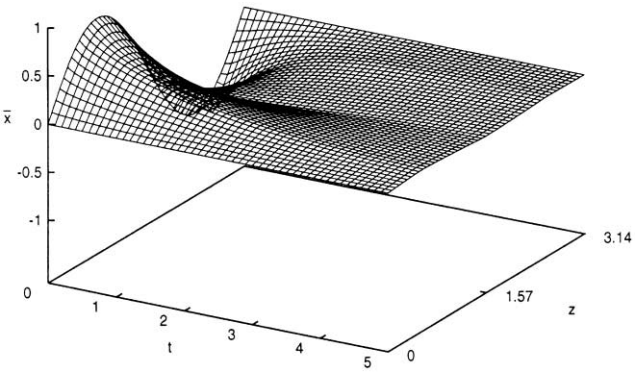

Fig. 14. Profile of evolution of the temperature of the rod, for the three actuator/sensor example, under output feedback control, for the optimal actuator/sensor locations, for $x_s(0) = \phi_2$.

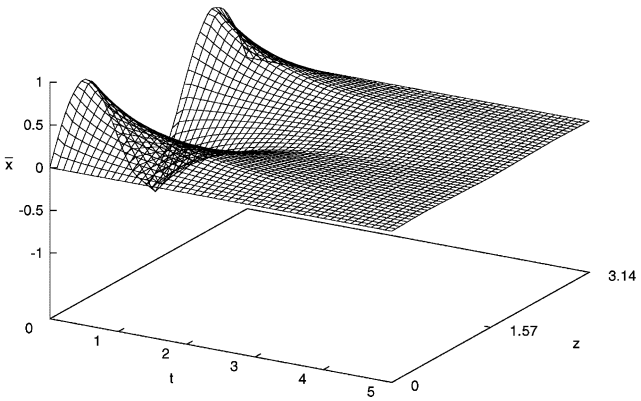

Fig. 15. Profile of evolution of the temperature of the rod, for the three actuator/sensor example, under output feedback control, for the optimal actuator/sensor locations, for $x_s(0) = \phi_3$.

and for $x_s(0) = \phi_3$ (Fig. 15). We can see that the proposed controller with optimal actuator/sensor locations, stabilizes the system to the spatially uniform operating steady state very quickly, for all three cases.

7. Application to a nonisothermal tubular reactor with recycle

We consider a nonisothermal tubular reactor shown in Fig. 16, where an irreversible first-order reaction of the form $A \rightarrow B$ takes place. The reaction is exothermic and a cooling jacket is used to remove heat from the reactor. The outlet of the reactor is fed to a separator where the unreacted species A is separated from the product B. The unreacted amount of species A is then fed back to the reactor through a recycle loop. Under standard modeling assumptions, the dynamic model of the process can be derived from mass and energy balances and takes the following dimensionless form

$$\frac{\partial \bar{x}_1}{\partial t} = -\frac{\partial \bar{x}_1}{\partial z} + \frac{1}{Pe_T}\frac{\partial^2 \bar{x}_1}{\partial z^2} + B_T B_C \exp^{\gamma \bar{x}_1/(1+\bar{x}_1)}(1+\bar{x}_2) + \beta_T(b(z)u(t) - \bar{x}_1), \tag{40}$$

$$\frac{\partial \bar{x}_2}{\partial t} = -\frac{\partial \bar{x}_2}{\partial z} + \frac{1}{Pe_C}\frac{\partial^2 \bar{x}_2}{\partial z^2} - B_C \exp^{\gamma \bar{x}_1/(1+\bar{x}_1)}(1+\bar{x}_2),$$

subject to the boundary conditions:

$$\frac{\partial \bar{x}_1(0,t)}{\partial z} = Pe_T(\bar{x}_1(0,t) - (1-r)\bar{x}_{1f}(t) - r\bar{x}_1(1,t)),$$

$$\frac{\partial \bar{x}_2(0,t)}{\partial z} = Pe_C(\bar{x}_2(0,t) - (1-r)\bar{x}_{2f}(t) - r\bar{x}_2(1,t)),$$

$$\frac{\partial \bar{x}_1(1,t)}{\partial z} = 0, \quad \frac{\partial \bar{x}_2(1,t)}{\partial z} = 0, \tag{41}$$

where $\bar{x}_1$ and $\bar{x}_2$ denote dimensionless temperature and concentration of species A in the reactor, respectively, $\bar{x}_{1f}$ and $\bar{x}_{2f}$ denote dimensionless inlet temperature and inlet concentration of species A in the reactor, respectively, Pe_T and Pe_C are the heat and thermal Peclet numbers, respectively, B_T and B_C denote a dimensionless heat of reaction and a dimensionless pre-exponential factor, respectively, r is the recirculation coefficient (it varies from zero to one, with one corresponding to total recycle and zero fresh feed and zero corresponding to no recycle), γ is a dimensionless activation energy, β_T is a dimensionless heat transfer coefficient, u is a dimensionless jacket temperature (chosen to be the manipulated input), and $b(z)$ is the actuator distribution function. Note here that for the purposes of this analysis, we will assume that there is no recycle loop dead time.

In order to transform the boundary condition of Eq. (41) to a homogeneous one, we insert the nonhomogeneous part of the boundary condition into the differential equation and obtain the following PDE representation of the process:

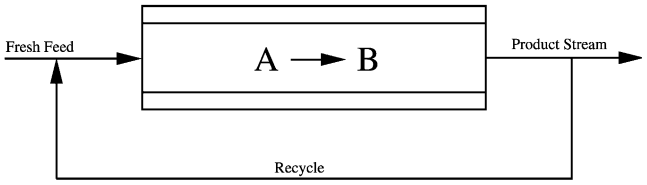

Fig. 16. A tubular reactor with recycle.

$$\frac{\partial \bar{x}_1}{\partial t} = -\frac{\partial \bar{x}_1}{\partial z} + \frac{1}{Pe_T}\frac{\partial^2 \bar{x}_1}{\partial z^2} + B_T B_C \exp^{\gamma \bar{x}_1/(1+\bar{x}_1)}(1+\bar{x}_2) + \beta_T(b(z)u(t) - \bar{x}_1) + \delta(z-0)((1-r)\bar{x}_{1f} + r\bar{x}_1(1,t)),$$

$$\frac{\partial \bar{x}_2}{\partial t} = -\frac{\partial \bar{x}_2}{\partial z} + \frac{1}{Pe_C}\frac{\partial^2 \bar{x}_2}{\partial z^2} - B_C \exp^{\gamma \bar{x}_1/(1+\bar{x}_1)}(1+\bar{x}_2) + \delta(z-0)((1-r)\bar{x}_{2f} + r\bar{x}_2(1,t)), \tag{42}$$

where $\delta(\cdot)$ is the standard Dirac function, subject to the homogeneous boundary conditions:

$$\frac{\partial \bar{x}_1(0,t)}{\partial z} = Pe_T\bar{x}_1(0,t), \quad \frac{\partial \bar{x}_2(0,t)}{\partial z} = Pe_C\bar{x}_2(0,t),$$

$$\frac{\partial \bar{x}_1(1,t)}{\partial z} = 0, \quad \frac{\partial \bar{x}_2(1,t)}{\partial z} = 0. \tag{43}$$

The following values for the process parameters were used in our calculations:

$$Pe_T = 7.0, \quad Pe_C = 7.0, \quad B_C = 0.1, \quad B_T = 2.5,$$

$$\beta_T = 2.0, \quad \gamma = 10.0, \quad r = 0.5, \quad \alpha = 5.0. \tag{44}$$

For the above values, the operating steady state of the open-loop system is unstable (the linearization around the steady state possesses one real unstable eigenvalue, $\mu = 0.0328$, and infinitely many stable eigenvalues), thereby implying the need to operate the process under feedback control. We note that in the absence of recycle loop (i.e., $r = 0$), the above process parameters correspond to a stable steady state for the open-loop system.

The spatial differential operator of the system of Eq. (42) is of the form

$$\mathscr{A}\bar{x} = \begin{bmatrix} \mathscr{A}_1\bar{x}_1 & 0 \\ 0 & \mathscr{A}_2\bar{x}_2 \end{bmatrix} = \begin{bmatrix} \dfrac{1}{Pe_T}\dfrac{\partial^2 \bar{x}_1}{\partial z^2} - \dfrac{\partial \bar{x}_1}{\partial z} & 0 \\ 0 & \dfrac{1}{Pe_C}\dfrac{\partial^2 \bar{x}_2}{\partial z^2} - \dfrac{\partial \bar{x}_2}{\partial z} \end{bmatrix}. \tag{45}$$

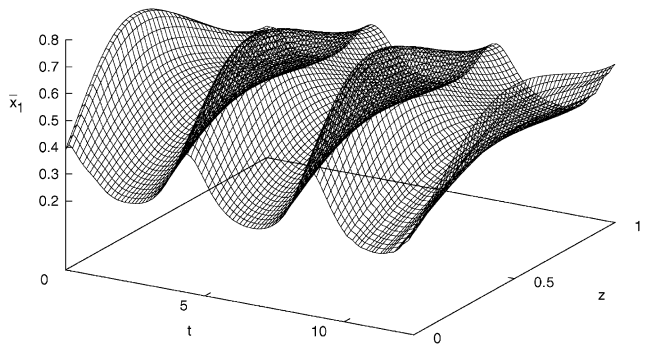

Fig. 17. Spatiotemporal evolution of $\bar{x}_1$ in the open-loop system.

The solution of the eigenvalue problem for $\mathscr{A}_i$ can be obtained by utilizing standard techniques from linear operator theory (see, for example, Ray (1981)) and is of the form

$$\lambda_{ij} = \frac{\bar{a}_{ij}^2}{Pe} + \frac{Pe}{4}, \quad i = 1,2, \ \ j = 1,\ldots,\infty,$$

$$\phi_{ij}(z) = B_{ij} e^{Pez/2}\left(\cos(\bar{a}_{ij}z) + \frac{Pe}{2\bar{a}_{ij}}\sin(\bar{a}_{ij}z)\right), \quad i = 1,2, \ \ j = 1,\ldots,\infty,$$

$$\bar{\phi}_{ij}(z) = e^{-Pez}\phi_{ij}(z), \quad i = 1,2, \ \ j = 1,\ldots,\infty, \tag{46}$$

where $Pe = Pe_T = Pe_C$, and $\lambda_{ij}, \phi_{ij}, \bar{\phi}_{ij}$, denote the eigenvalues, eigenfunctions and adjoint eigenfunctions of $\mathscr{A}_i$, respectively. $\bar{a}_{ij}, B_{ij}$ can be calculated from the following formulas:

$$\tan(\bar{a}_{ij}) = \frac{Pe\bar{a}_{ij}}{\bar{a}_{ij}^2 - (\frac{Pe}{2})^2}, \quad i = 1,2, \ \ j = 1,\ldots,\infty$$

$$B_{ij} = \left\{\int_0^1 \left(\cos(\bar{a}_{ij}z) + \frac{Pe}{2\bar{a}_{ij}}\sin(\bar{a}_{ij}z)\right)^2 dz\right\}^{-1/2}, \tag{47}$$

$$i = 1,2, \ \ j = 1,\ldots,\infty.$$

A 400th order Galerkin truncation of the system of Eqs. (42)–(44) was used in our simulations in order to accurately describe the process (further increase on the order of the Galerkin truncation was found to give negligible improvement on the accuracy of the results). Fig. 17 shows the open-loop profile of $\bar{x}_1$ along the length of the reactor, which corresponds to the operating unstable steady-state. Therefore, the control problem is to manipulate the wall temperature, $u(t)$, in order to stabilize the reactor at the desired operating steady-state, and the control output was defined as $y_c(t) = \int_0^1 e^{-Pez}\phi_{11}(z)x_{11}\,dz$. The process was initially ($t = 0$) assumed to be at the unstable steady state, and the desired reference input value was set at $v = 0.12$.

Based on simulations of the open-loop process dynamics, we take as the slow modes of the process the first eight temperature modes plus the first thirty concentration modes and use Galerkin's method to derive a 38th-order ODE system employed for controller synthesis. We use one control actuator to stabilize the system (note that this is possible since the assumption $m = l$ is sufficient and not necessary; see also discussion in Remark 3), and the actuator distribution function was taken to be $b(z) = \delta(z - z_{act})$ (one point control actuator placed at $z = z_{act}$). Since it is not feasible in practice to measure the concentration of species A in the reactor at 30 spatial positions, we use eight point temperature sensors to obtain estimates of the first eight modes of the reactor temperature (i.e., the measurement sensor shape function takes the form $s(z) = [\delta(z - z_{s1}) \ \ \delta(z - z_{s2}) \ \ \ldots \ \ \delta(z - z_{s8})]^T$) and design a nonlinear Luenberger-type state observer consisting of 30 ordinary differential equations to obtain estimates of the first 30 concentration modes from the temperature measurements (see, for example, Christofides (1998) for details on how such an observer can be designed).

Since the process is initially ($t = 0$) assumed to be at the unstable steady state, we will compute the optimal location of control actuator and measurement sensors with respect to this initial condition. Furthermore, since the reference input value is set at $v = 0.12$, we define the costs J, J_x, and J_u as follows:

$$\begin{aligned} J &= J_x + J_u \\ &= \int_0^\infty ((x_s - x_{sf})^T Q_s (x_s - x_{sf}) \\ &\quad + (x_f - x_{ff})^T Q_f (x_f - x_{ff}))\,dt \\ &\quad + \int_0^\infty (u - u_f)^T R (u - u_f)\,dt, \end{aligned} \tag{48}$$

where x_{sf}, x_{ff}, and u_f are the values of x_s, x_f, and u, respectively, at the desired operating steady state, to ensure that the costs become zero when the process is stabilized at the steady state. Table 5 shows the values of the costs J_u, J_x, and J for state feedback control, in the case of optimal actuator placement, and for the sake of comparison, the values of these costs in the case of alternative actuator placements. Fig. 18 shows the control action u, for the optimal case (solid line), case 2 (long-dashed line), case 3 (short-dashed line), case 4 (dotted line), and case 5 (dashed-dotted line). Clearly, the control action spent to stabilize the system at the desired operating profile in

Table 5
Results for different actuator location

Case	Actuator location	$J_u(10^{-5})$	$J_x(10^{-5})$	$J(10^{-5})$
Optimal	0	9.647	36.536	46.183
2	0.1	21.540	36.536	58.076
3	0.2	60.062	36.536	96.598
4	0.3	229.42	36.536	265.95
5	0.4	1,672.8	36.536	1,709.3

Table 6
Results for different sensor locations

Case	Sensor locations	$J_u(10^{-5})$	$J_x(10^{-5})$	$J(10^{-5})$
1	0.05, 0.15, 0.30, 0.45, 0.55, 0.70, 0.85, 0.95	10.280	39.717	49.997
2	0.07, 0.20, 0.32, 0.44, 0.56, 0.68, 0.80, 0.93	10.029	38.099	48.128
3	0.05, 0.20, 0.35, 0.45, 0.55, 0.65, 0.80, 0.95	10.096	39.011	49.107
4	0.06, 0.18, 0.31, 0.43, 0.56, 0.68, 0.81, 0.93	9.748	36.446	46.194

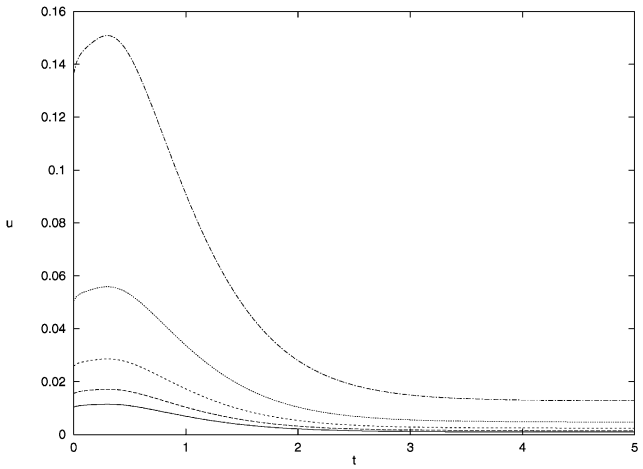

Fig. 18. Closed-loop control effort, u, for the optimal actuator location at $z_{act}=0$ (solid line), for the actuator location at $z_{act}=0.1$ (long-dashed line), at $z_{act}=0.2$ (short-dashed line), at $z_{act}=0.3$ (dotted line), and at $Z_{act}=0.4$ (dashed-dotted line).

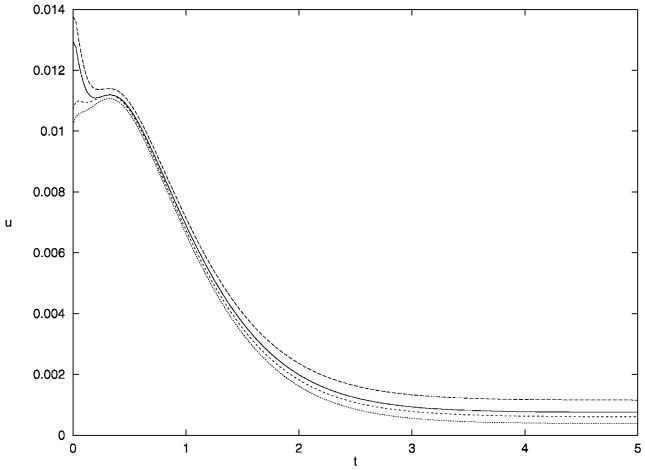

Fig. 19. Closed-loop control effort, u, for four different sensor locations; case 1 (solid line), case 2 (long-dashed line), case 3 (short-dashed line), and case 4 (dotted line).

the case of optimal actuator placement at $z_{act}=0$, is significantly less than the other four cases.

We now proceed with the output feedback implementation of the state feedback controller. To this end, we pick the sensors locations so that the resulting output feedback controller guarantees stability of the closed-loop system and the estimation error in the closed-loop system is very small. Table 6 shows values of the costs J_u, J_x, and J for four different sensor locations. Figs. 19 and 20 show the profile of the control action u, and the final steady-state profile of $\bar{x}_1$, for case 1 (solid line), case 2 (long-dashed line), case 3 (short-dashed line), and case 4 (dotted line). Clearly, in all these cases, the stabilization of the unstable steady state is achieved with comparable cost, thereby indicating that 8 pint temperature sensors distributed appropriately along the length of the reactor suffice to obtain a stabilizing output feedback controller. To demonstrate the performance of the controller, Fig. 21 shows the evolution of the closed-loop reactor temperature for the optimal actuator locations and for the sensor location of case 1. The controller stabilizes the process very close to the desired operating profile.

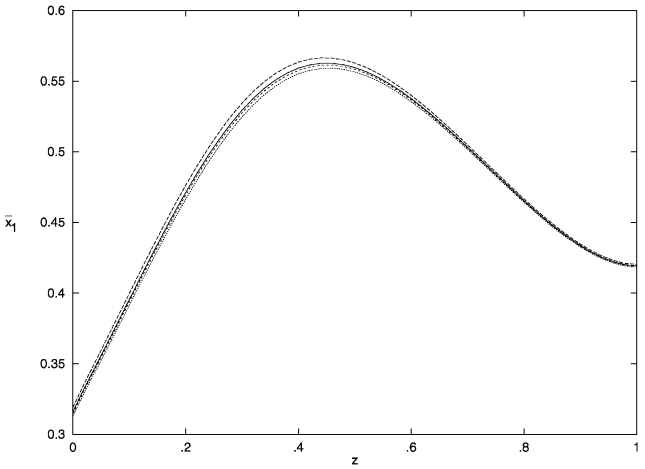

Fig. 20. Final steady-state profile of $\bar{x}_1$, for four different sensor locations; case 1 (solid line), case 2 (long-dashed line), case 3 (short-dashed line), and case 4 (dotted line).

Remark 8. Referring to the above examples, we note that the optimal sensor locations depend significantly on the choice of boundary conditions and the location of the control actuators. When the process states at the boundaries are fixed at a constant value (Dirichlet-type boundary conditions), the sensors are placed away from the boundaries since we cannot gain much information about the system behavior by placing the sensors close to the boundaries. On the other hand, if the boundary conditions are of mixed type (Robin-type boundary conditions), the states of the system close to the boundaries significantly

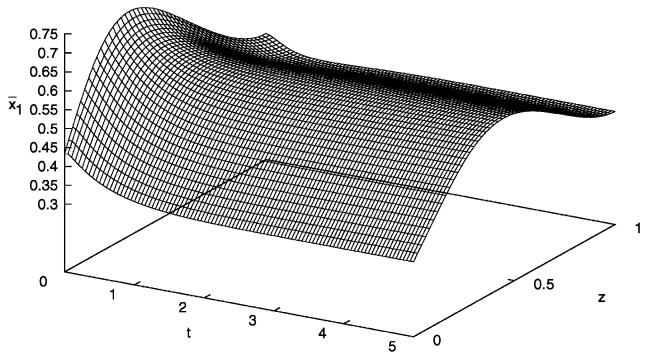

Fig. 21. Spatiotemporal evolution of $\bar{x}_1$ under the nonlinear output feedback controller with the optimally placed actuator, and the first configuration for the locations of the sensors.

change with time, and thus, measurements close to the boundaries provide more information about the dynamics of the system. In addition, the sensors should be placed away from the actuator locations in order to obtain more information about the dynamics of the system, since on and near the control actuators the state of the system is affected more by the dynamics of the controller and less by the dynamics of the process.

Remark 9. Referring to the design of the gain of the nonlinear Luenberger-type state observer used to obtain estimates of the first 30 concentration modes from the temperature measurements, we note that the gain was chosen so that the poles of the linearization of the observer are stable (i.e., they lie in the left-half of the complex plane) and close in magnitude to the slow eigenvalues of the linearized open-loop process. This was done to make sure that the state observer does not introduce additional fast dynamics (as, for example, would be the case if we were using an observer whose poles were of the order $1/\varepsilon$), which could perturb the separation of the slow and fast modes of the open-loop PDE system.

8. Conclusions

In this work, we proposed a general and practical methodology for the integration of nonlinear output feedback control with optimal placement of control actuators and measurement sensors for transport-reaction processes described by a broad class of quasi-linear parabolic PDEs. Given a class of stabilizing nonlinear state feedback controllers which were derived on the basis of finite-dimensional approximations of the PDE, the optimal actuator location problem was formulated as the one of minimizing a meaningful cost functional that includes penalty on the response of the closed-loop system and the control action and was solved by using standard unconstrained optimization techniques. Then, under the assumption that the number of measurement sensors is equal to the number of slow modes, estimates for the states of the approximate finite-dimensional model from the measurements were computed and used to derive nonlinear output feedback controllers. The optimal location of the measurement sensors was computed by minimizing a cost function of the estimation error in the closed-loop infinite-dimensional system. It was rigorously established that the proposed output feedback controllers enforce stability in the closed-loop infinite-dimensional system and that the solution to the optimal actuator/sensor problem, which is obtained on the basis of the closed-loop finite-dimensional system, is near-optimal in the sense that it approaches the optimal solution for the infinite-dimensional system as the separation of the slow and fast eigenmodes increases. The proposed methodology was successfully applied to a diffusion-reaction process and a non-isothermal tubular reactor with recycle to derive nonlinear output feedback controllers and compute optimal actuator/sensor locations for stabilization of unstable steady-states.

Acknowledgements

Financial support from NSF, CTS-0002626, is gratefully acknowledged.

Appendix A.

A.1. Proof of Theorem 1

The proof of this theorem will be obtained in two steps. In the first step, we will show exponentially stability and closeness of solutions for the closed-loop system of Eq. (11), provided that the initial conditions and ε are sufficiently small. In the second step, we will exploit the closeness of solutions result to show that the cost associated with the closed-loop PDE system approaches the optimal cost associated with the closed-loop finite-dimensional system under state feedback control, when the initial conditions and ε are sufficiently small, thereby establishing that the location of the control actuators obtained by using the finite-dimensional system is near-optimal.

Exponential stability—closeness of solutions: Using that $\varepsilon = |Re\,\lambda_1|/|Re\,\lambda_{m+1}|$ and under the controller of Eq. (15), the closed-loop system of Eq. (11) takes the form

$$\begin{aligned} \frac{dx_s}{dt} &= A_s x_s + f_s(x_s, x_f) - f_s(x_s, 0), \\ \varepsilon \frac{\partial x_f}{\partial t} &= \mathcal{A}_{f\varepsilon} x_f + \varepsilon \bar{f}_f(x_s, x_f), \end{aligned} \tag{A.1}$$

where $\mathscr{A}_{f\varepsilon}$ is an unbounded differential operator defined as $\mathscr{A}_{f\varepsilon}=\varepsilon\mathscr{A}_f$, and $\bar{f}_f(x_s,x_f)=\mathscr{B}_f\mathscr{B}_s^{-1}((\mathscr{A}_s-\Lambda_s)x_s+f_s(x_s,0))+f_f(x_s,x_f)$. Since ε is a small positive number less than unity (Assumption 1, part 3), the system of Eq. (A.1) is in the standard singularly perturbed form, with x_s being the slow states and x_f being the fast states. Introducing the fast time scale $\tau=t/\varepsilon$ and setting $\varepsilon=0$, we obtain the following infinite-dimensional fast subsystem from the system of Eq. (A.1):

$$\frac{\partial\tilde{x}_f}{\partial\tau}=\mathscr{A}_{f\varepsilon}\tilde{x}_f, \tag{A.2}$$

where the tilde symbol in $\tilde{x}_f$, denotes that the state $\tilde{x}_{cf}$ is associated with the approximation of the fast x_f-subsystem. From the fact that $Re\,\lambda_{m+1}<0$ and the definition of ε, we have that the above system is globally exponentially stable. Setting $\varepsilon=0$ in the system of Eq. (A.1) and using that the operator $\mathscr{A}_{f\varepsilon}$ is invertible, we have that

$$\tilde{x}_f=0, \tag{A.3}$$

and thus the closed-loop of the finite-dimensional slow system takes the form

$$\frac{\mathrm{d}\tilde{x}_s}{\mathrm{d}t}=\Lambda_s\tilde{x}_s. \tag{A.4}$$

The above slow subsystem is globally exponentially stable since Λ_s is a stable matrix. From the fact that the slow subsystem of Eq. (A.4) and the fast subsystem of Eq. (A.2) are globally exponentially stable, there exist positive real numbers μ_1,μ_2, and ε^* such that if $|x_s(t)|\leqslant\mu_1$, $\|x_f(t)\|_2\leqslant\mu_2$, and $\varepsilon\in(0,\varepsilon^*]$, then the system of Eq. (A.1) is exponentially stable and the solution $x_s(t),x_f(t)$ of the system of Eq. (A.1) satisfies for all $t\in[t_b,\infty)$:

$$\begin{aligned}x_s(t)&=\tilde{x}_s(t)+O(\varepsilon),\\ x_f(t)&=\tilde{x}_f(t)+O(\varepsilon),\end{aligned} \tag{A.5}$$

where t_b is the time required for $x_f(t)$ to approach $\tilde{x}_f(t)$. $\tilde{x}_s(t)$ and $\tilde{x}_f(t)$ are the solutions of the slow and fast subsystems of Eq. (A.2) and Eq. (A.4) respectively ([10], Proposition 1).

Near-optimality of the actuator locations: The cost for the closed-loop infinite-dimensional system can be written as follows:

$$\begin{aligned}\hat{J}=\frac{1}{m}\sum_{i=1}^{m}\int_0^{t_b}&((x_s^{\mathrm{T}}(x_s^i(0),t),Q_sx_s(x_s^i(0),t))\\&+(x_f^{\mathrm{T}}(x_s^i(0),t),Q_fx_f(x_f^i(0),t))\\&+u^{\mathrm{T}}(x_s(x_s^i(0),t),z_a)Ru(x_s(x_s^i(0),t),z_a))\,\mathrm{d}t\\&+\frac{1}{m}\sum_{i=1}^{m}\int_{t_b}^{\infty}((x_s^{\mathrm{T}}(x_s^i(0),t),Q_sx_s(x_s^i(0),t))\\&+(x_f^{\mathrm{T}}(x_s^i(0),t),Q_fx_f(x_f^i(0),t))\\&+u^{\mathrm{T}}(x_s(x_s^i(0),t),z_a)Ru(x_s(x_s^i(0),t),z_a))\,\mathrm{d}t.\end{aligned} \tag{A.6}$$

It follows then from the continuity properties of the state $x(t)$ and the control $u(t)$ that for all $t\geqslant t_b$ and $i=1,\ldots,m$:

$$\begin{aligned}&x_s(x_s^i(0),t)\to\tilde{x}_s(x_s^i(0),t),\quad x_f(x_f^i(0),t)\to0,\\&u(x_s(x_s^i(0),t),z_a)\to u(\tilde{x}_s(x_s^i(0),t),z_a)\quad\text{as }\varepsilon\to0\end{aligned} \tag{A.7}$$

and hence

$$\begin{aligned}&\frac{1}{m}\sum_{i=1}^{m}\int_{t_b}^{\infty}(x_s^{\mathrm{T}}(x_s^i(0),t)Q_sx_s(x_s^i(0),t)\\&\quad+(x_f^{\mathrm{T}}(x_f^i(0),t)Q_fx_f(x_f^i(0),t)\\&\quad+u^{\mathrm{T}}(x_s(x_s^i(0),t),z_a)Ru(x_s(x_s^i(0),t),z_a))\,\mathrm{d}t\\&\quad\to\frac{1}{m}\sum_{i=1}^{m}\int_{t_b}^{\infty}(\tilde{x}_s^{\mathrm{T}}(x_s^i(0),t)Q_s\tilde{x}_s(x_s^i(0),t)\\&\qquad+u^{\mathrm{T}}(\tilde{x}_s(x_s^i(0),t),z_a)\\&\qquad Ru(\tilde{x}_s(x_s^i(0),t),z_a))\,\mathrm{d}t\quad\text{as }\varepsilon\to0.\end{aligned} \tag{A.8}$$

From the exponential stability of the closed-loop system, we have that there exists a positive real number M that bounds the integrand of Eq. (A.6). Using the fact that $t_b=O(\varepsilon)$, we then have

$$\begin{aligned}&\frac{1}{m}\sum_{i=1}^{m}\int_0^{t_b}(x_s^{\mathrm{T}}(x_s^i(0),t)Q_sx_s(x_s^i(0),t)\\&\quad+(x_f^{\mathrm{T}}(x_f^i(0),t)Q_fx_f(x_f^i(0),t)\\&\quad+u^{\mathrm{T}}(x_s(x_s^i(0),t),z_a)Ru(x_s(x_s^i(0),t),z_a))\,\mathrm{d}t\\&\quad\leqslant\int_0^{t_b}M\,\mathrm{d}t\\&\quad\leqslant M\varepsilon\\&\quad=O(\varepsilon).\end{aligned} \tag{A.9}$$

Similarly, from the stability of the closed-loop finite-dimensional system of Eq. (12) and the fact that $t_b=O(\varepsilon)$, we have that there exists a positive real number M' such that

$$\begin{aligned}&\frac{1}{m}\sum_{i=1}^{m}\int_0^{t_b}(\tilde{x}_s^{\mathrm{T}}(x_s^i(0),t)Q_s\tilde{x}_s(x_s^i(0),t)\\&\quad+u^{\mathrm{T}}(\tilde{x}_s(x_s^i(0),t),z_a)Ru(\tilde{x}_s(x_s^i(0),t),z_a))\,\mathrm{d}t\\&\quad\leqslant\int_0^{t_b}M'\,\mathrm{d}t\\&\quad\leqslant M'\varepsilon\\&\quad=O(\varepsilon).\end{aligned} \tag{A.10}$$

Combining Eqs. (A.8)–(A.10), we obtain

$$\frac{1}{m}\sum_{i=1}^{m}\int_{t_b}^{\infty}(x_s^{\mathrm{T}}(x_s^i(0),t)Q_s x_s(x_s^i(0),t) + (x_f^{\mathrm{T}}(x_f^i(0),t)Q_f x_f(x_f^i(0),t) + u^{\mathrm{T}}(x_s(x_s^i(0),t),z_a)Ru(x_s(x_s^i(0),t),z_a))\,\mathrm{d}t \to \frac{1}{m}\sum_{i=1}^{m}\int_{t_b}^{\infty}(\tilde{x}_s^{\mathrm{T}}(x_s^i(0),t)Q_s\tilde{x}_s(x_s^i(0),t) + u^{\mathrm{T}}(\tilde{x}_s(x_s^i(0),t),z_a)Ru(\tilde{x}_s(x_s^i(0),t),z_a))\,\mathrm{d}t \quad \text{as } \varepsilon\to 0. \tag{A.11}$$

This completes the proof of the theorem. □

A.2. Proof of Theorem 2

Under the output feedback controller of Eq. (24), the closed-loop system takes the form

$$\frac{\mathrm{d}x_s}{\mathrm{d}t} = \Lambda_s x_s + (\mathscr{A}_s - \Lambda_s)x_f + f_s(x_s,x_f) - f_s(x_s+x_f,0),$$
$$\varepsilon\frac{\partial x_f}{\partial t} = \mathscr{A}_{f\varepsilon}x_f + \varepsilon\mathscr{B}_f\mathscr{B}_s^{-1}((\mathscr{A}_s-\Lambda_s)(x_s+x_f) + f_s(x_s+x_f,0)) + \varepsilon f_f(x_s,x_f). \tag{A.12}$$

Using that ε is a small positive number less than unity (Assumption 1, part 3), and introducing the fast time-scale $\tau = t/\varepsilon$ and setting $\varepsilon = 0$, we obtain the following infinite-dimensional fast subsystem which describes the fast dynamics of the system of Eq. (A.12)

$$\frac{\partial\tilde{x}_f}{\partial\tau} = \mathscr{A}_{f\varepsilon}\tilde{x}_f, \tag{A.13}$$

which is globally exponentially stable. Setting $\varepsilon = 0$ in the system of Eq. (A.12) and using that the operator $\mathscr{A}_{f\varepsilon}$ is invertible, we have that

$$\tilde{x}_f = 0 \tag{A.14}$$

and thus the closed-loop of the finite-dimensional slow system takes the form

$$\frac{\mathrm{d}\tilde{x}_s}{\mathrm{d}t} = \Lambda_s\tilde{x}_s. \tag{A.15}$$

From the fact that the slow subsystem of Eq. (A.15) and the fast subsystem of Eq. (A.2) are globally exponentially stable, there exist positive real numbers μ_1, μ_2, and ε^* such that if $|x_s(t)| \leqslant \mu_1$, $\|x_f(t)\|_2 \leqslant \mu_2$, and $\varepsilon \in (0,\varepsilon^*]$, then the system of Eq. (A.1) is exponentially stable and the solution $x_s(t)$, $x_f(t)$ of the system of Eq. (A.12) satisfies the estimates of Eq. (A.15).

Given the stability and closeness of solutions results for the closed-loop system, the near-optimality of the control actuators and measurement sensors in the sense described in Eq. (25) can be established by using similar calculations to the ones in part 2 of the proof of Theorem 1. □

References

Alvarez, J., Romagnoli, J. A., & Stephanopoulos, G. (1981). Variable measurement structures for the control of a tubular reactor. *Chemical Engineering Science*, *36*, 1695–1712.

Amouroux, M., Di Pillo, G., & Grippo, L. (1976). Optimal selection of sensors and control location for a class of distributed parameter systems. *Ricerca Automatica*, *7*, 92.

Arbel, A. (1981). Controllability measures and actuator placement in oscillatory systems. *International Journal of Control*, *33*, 565–574.

Balas, M. J. (1979). Feedback control of linear diffusion processes. *International Journal of Control*, *29*, 523–533.

Chen, W. H., & Seinfeld, J. H. (1975). Optimal location of process measurements. *International Journal of Control*, *21*, 1003–1014.

Choe, K., & Baruh, H. (1992). Actuator placement in structural control. *Journal of Guidance*, *15*, 40–48.

Christofides, P. D. (1998). Output feedback control of nonlinear two-time-scale processes. *Industrial and Engineering Chemistry Research*, *37*, 1893–1909.

Christofides, P. D. (2001). *Nonlinear and robust control of PDE systems: Methods and applications to transport-reaction processes*. Boston: Birkhäuser.

Christofides, P. D., & Baker, J. (1999). Robust output feedback control of quasi-linear parabolic PDE systems. *Systems & Control Letters*, *36*, 307–316.

Christofides, P. D., & Daoutidis, P. (1997). Finite-dimensional control of parabolic PDE systems using approximate inertial manifolds. *Journal of Mathematical Analysis and Applications*, *216*, 398–420.

Colantuoni, G., & Padmanabhan, L. (1977). Optimal sensor locations for tubular-flow reactor systems. *Chemical Engineering Science*, *32*, 1035–1049.

Courdesses, M. (1978). Optimal sensors and controllers allocation in output feedback control for a class of distributed parameter systems, *Proceedings of the symposium on advances in measurement & control*, Athens (pp. 735–740).

Demetriou, M. A. (1999). Numerical investigation on optimal actuator/sensor location of parabolic PDEs. *Proceedings of the American control conference*, San Diego, CA (pp. 1722–1726).

Friedman, A. (1976). *Partial differential equations*. New York: Holt, Rinehart & Winston.

Harris, T. J., MacGregor, J. F., & Wright, J. D. (1980). Optimal sensor location with an application to a packed bed tubular reactor. *A.I.Ch.E. Journal*, *26*, 910–916.

Ichikawa, A., & Ryan, E. P. (1977). Filtering and control of distributed parameter systems with point observations and inputs. *Proceedings of second IFAC symposium on control of D.P.S.*, Coventry. (pp. 347–357).

Isidori, A. (1989). *Nonlinear control systems: An introduction.* (2nd ed.). Berlin-Heidelberg: Springer.

Kubrusly, C. S., & Malebranche, H. (1985). Sensors and controllers location in distributed systems—a survey. *Automatica*, *21*, 117–128.

Kumar, S., & Seinfeld, J. H. (1978a). Optimal location of measurements for distributed parameter estimation. *IEEE Transactions on Automatic Control*, *23*, 690–698.

Kumar, S., & Seinfeld, J. H. (1978b). Optimal location of measurements in tubular reactors. *Chemical Engineering Science*, *33*, 1507–1516.

Levine, W. S., & Athans, M. (1978). On the determination of the optimal constant output feedback gains for linear multivariable system. *IEEE Transactions on Automatic Control*, *15*, 44–48.

Malandrakis, C. G. (1979). Optimal sensor and controller allocation for a class of distributed parameter systems. *International Journal of Systems Science*, *10*, 1283.

Morari, M., & O'Dowd, M. J. (1980). Optimal sensor location in the presence of nonstationary noise. *Automatica*, *16*, 463–480.

Omatu, S., Koide, S., & Soeda, T. (1978). Optimal sensor location problem for a linear distributed parameter system. *IEEE Transactions on Automatic Control*, *AC-23*, 665–673.

Omatu, S., & Seinfeld, J. H. (1983). Optimization of sensor and actuator location in a distributed parameter system. *Journal of the Franklin Institute*, *315*, 407–421.

Rao, S. S., Pan, T. S., & Venkayya, V. B. (1991). Optimal placement of actuators in actively controlled structures using genetic algorithms. *AIAA Journal*, *29*, 942–943.

Ray, W. H. (1981). *Advanced process control*. New York: McGraw-Hill.

Waldraff, W., Dochain, D., Bourrel, S., & Magnus, A. (1998). On the use of observability measures for sensor location in tubular reactor. *Journal of Process Control*, *8*, 497–505.

Xu, K., Warnitchai, P., & Igusa, T. (1994). Optimal placement and gains of sensors and actuators for feedback control. *Journal of Guidance, Dynamics and Control*, *17*, 929–934.

Yu, T. K., & Seinfeld, J. H. (1973). Observability and optimal measurement location in linear distributed parameter systems. *International Journal of Control*, *18*, 785–799.